Spatial vulnerability assessment of silver fir and Norway spruce dieback driven by climate warming

Christian Piedallu, Donatien Dallery, Célia Bresson, Myriam Legay, Jean-Claude Gégout, Rodolphe Pierrat

Spatial vulnerability assessment of silver fir and Norway spruce dieback driven by climate warming

Authors: Christian Piedallu[a*], Donatien Dallery[a], Célia Bresson[a], Myriam Legay[a], Jean-Claude Gégout[a], Rodolphe Pierrat [b]

[a] Université de Lorraine, AgroParisTech, INRAE, Silva, 54000 Nancy, France

[b] ONF, DT Grand-Est, cité administrative, 14, rue du Maréchal Juin, 37084 STRASBOURG Cedex

*Corresponding author, AgroParisTech - Centre de Nancy, 14 rue Girardet - CS 14216, 54042 NANCY Cedex France, email: christian.piedallu@agroparistech.fr, ORCID: 0000-0001-7316-1874

Abstract

Context: A significant forest decline has been noticed these last years in Europe. Managers need tools to better anticipate these massive events.

Objectives: We evaluated the efficiency of easily available data about environmental conditions and stand characteristics to determine different levels of vulnerability.

Methods: We combined remote sensing images, photo-interpretation, and digital models describing environmental conditions within a modelling approach to achieve spatial vulnerability assessment of the stands. We focused on silver fir and Norway spruce stands in the Vosges mountains (8,900 km², northeastern France), where severe symptoms of decline are visible.

Results: Silver fir were predicted highly vulnerable on 7% of their area *versus* 33% for Norway spruce. Using an independent dataset, we observed ten-times (silver fir) and two-times (Norway spruce) higher mortality rates in the units with a high level of vulnerability than in the others. About half of the model deviance was directly or indirectly explained by variables related to water stress (soils displaying low water availability, having suffered severe drying events these last years). Furthermore, the stands acclimatised to drought conditions were more resilient. Stand characteristics also influenced dieback spread, suggesting that an evolution of silvicultural practices toward mixed stands with broadleaved species and uneven-aged trees can contribute to better adapt to future climate conditions.

Conclusions: Vulnerability maps based on easily available geographic information describing climate, soil, and topography can efficiently discriminate canopy mortality patterns over broad areas, and can be useful tools for managers to mitigate the effects of climate change on forests.

Keywords: climate change, forest dieback, decline, drought, tree vulnerability, vulnerability map.

Introduction

With a global mean temperature increase of at least 1.1°C and changes in rainfall patterns, the effects of the ongoing climate change are more and more visible and consequential on ecosystem functioning (Pörtner et al. 2022). Increased tree mortality and changes in forest structure and composition have been observed in different biomes (Allen et al. 2015; Michel and Seidling 2018). In the western United States, van Mantgem et al. (2009) demonstrated a doubling of the rate of background tree mortality every 17 to 29 years, while Peng et al. (2011) observed a 4.9% increase in tree mortality per year from 1963 to 2008 in Canadian boreal forests. In Europe, remote sensing data have revealed a 2.4% increase of canopy mortality *per* year between 1984 and 2016 (Senf et al. 2018), and different hotspots have been identified in the north or the south of the continent (Neumann et al. 2017). These trends were most of the time attributed to the recent changes in climate (Han and Singh 2020; Senf et al. 2020). An excess of tree mortality has been associated to the current changes in temperature or rainfall for about half of the most common European tree species (Taccoen et al. 2019). The impact of climate change on forest decline is expected to persist in the future: climate projections predict that warming will continue, involving decreased water availability for plants and more extreme weather events (Pörtner et al. 2022).

Climate-related forest dieback is a major concern for forest ecosystems because it influences species composition and structure, affects forest carbon sequestration and water cycle regulation, soil protection, refugia for biodiversity, provision of forest products, recreational uses … (Brockerhoff et al. 2017). Forest dieback also has an effect on local or regional climate conditions by modifying the albedo and heat fluxes (Anderson et al. 2011). Despite the major importance of the issue, the way forests will cope with climate change remains highly uncertain. Vulnerability assessments are done *a posteriori* most of the time, and forest managers cannot anticipate

55 massive mortality events. The choice of the tree species – traditionally based on specific ecological requirements
56 – can no longer correspond to current climate conditions (Torssonen et al. 2015). In a context of increasing impacts
57 of recent droughts on ecosystems in a large part of Europe (Buras et al. 2020), evaluating the mortality risk across
58 broad areas is crucial to adapt management strategies to the new ecological conditions and make the forest more
59 resistant and resilient to ongoing changes (Bastin et al. 2019; Bonan 2008).

60

61 Species mortality is a natural component of the forest dynamics that can be increased by different stresses.
62 Tree decline is often described as a gradual process involving a combination of interchangeable predisposing,
63 inciting, and contributing factors that interact at different time and spatial scales (Sinclair, 1965), sometimes with
64 delayed effects (Lebourgeois 2007). This conceptual framework was popularised by the decline spiral in the 1980s
65 (Manion 1981). Predisposing factors reduce tree ability to withstand a stress on the long term. Tree growth leads
66 to overcrowding and natural mortality through self-thinning, particularly for suppressed trees or in high-density
67 stands (Charru et al. 2012). Predisposing factors are related to tree or stand characteristics (age, competition for
68 light, species interactions), but also poor site conditions (high temperature, low water availability, soil properties),
69 or air pollution (nitrogen, sulphur deposition, ozone) (Brandl et al. 2020; Dietze and Moorcroft 2011; Taccoen et
70 al. 2019). Inciting factors usually result from extreme events like drought, heat waves, frost, snow, forest fires,
71 floods, or storms (Maringer et al. 2021). The deleterious effects of droughts and heat waves on tree fitness are
72 probably the most extensively studied (Choat et al. 2012; Urli et al. 2013; Williams et al. 2013). Allen et al. (2010)
73 identified more than 150 references on forest mortality driven by extreme events since 1970. The impact of inciting
74 factors is expected to increase in the current climate change context (Hartmann et al. 2018; Schelhaas et al. 2003).
75 Contributing factors are often insects or pathogens that cause the final decline of the trees that have already suffered
76 from predisposing or inciting factors through hydraulic failure or carbon starvation (Maruini et al. 2017; McDowell
77 et al. 2008). Several recent outbreaks of bark beetles are considered as some of the most severe outbreaks ever
78 seen (Lundquist 2019). At the end of April 2019, the French National Forest Office (ONF) estimated that 60% of
79 spruce were affected by bark beetle attacks, *versus* 15% in the usual course of events (Office National des Forêts
80 2020[1]).

81

[1] https://www.onf.fr/+/4bd::ces-arbres-forestiers-qui-souffrent-de-la-secheresse.html

The decline of silver fir or Norway spruce in not new in Europe (Maringer et al. 2021). Northeastern France already experienced severe tree decline events during the last century, during the 1916-1925 or 1943-1951 periods for example. During this latter period, an up to 40 % decrease in radial growth of silver fir was attributed to drought (Becker 1987). The 1973-1981 period was also marked by another important crisis. After Germany and many countries of central Europe, severe decline was observed on several thousand hectares in the Vosges mountains (Bouvarel 1984). In 1984, an observatory network recorded that 26% of silver fir, 20 % of Scot pine and 17% of Norway spruce had lost more 20% of their needles. More mortality was observed on old trees in the east of the mountain range, and on acidic substratum whatever the altitude (Bonneau 1985; Thomas et al. 2002). Climatic stress after the 1976 drought and air pollution that increased the nutritional difficulties and led to magnesium deficiencies were identified as the main drivers of this forest decline (Elling et al. 2009; Landmann et al. 1987; Vitali et al. 2017). Following the reduction in SO_2 concentrations in the air and a period with more suitable climatic conditions, strong recovery was observed after 1981 (Lévy 1987). Tree decline was observed again more recently, mainly on Norway spruce and silver fir, after important drought events followed by an increase of bark beetle attacks, as in 2003 (Ciais et al. 2005) or 2018 (Buras et al. 2020). Silver fir and Norway spruce have been gradually declining in Europe since 2016, questioning managers and policy makers about the future of these species (Obladen et al. 2021). In 2019, Norway spruce represented 32 % of damage at the European scale, with an estimated wood loss of approximatively 36 million m^3. The countries of central Europe were most affected. Although forest decline has been extensively studied, the causes of mortality and the ecological limits of the species that trigger mortality are not well understood, and this restrains our capacity to consider the risk of dieback in forest management.

The vulnerability assessment evaluates the ability of a tree or a forest stand to tolerate a stress. The level of vulnerability varies according to the species sensitivity (its capacity to resist to changing climate), local exposure (related to the intensity of the effects of climate change), and the adaptive capacity of the species (its ability to cope with the new climate conditions) (McCarthy et al. 2001). Different approaches have been implemented for managers to facilitate forest adaptation to the new climatic conditions, e.g., recommendations by expert knowledge according to site type maps, or more sophisticated vulnerability assessment based on large databases from forest inventories or remote sensing data, coupled with mechanistic or statistical models. One of the most popular approaches is based on empirical niche models or process-based models (Coops and Waring

2011; Fremout et al. 2020). It simulates the suitable areas of the species according to contemporary or simulated climate. These models can be used to evaluate if the species can maintain itself under warmer climate conditions, or to track their current climate niche (Aubin et al. 2018). They have important limitations because the numerous assumptions often lead to overestimating the risk (Das et al. 2022). Vulnerability can also be estimated by modelling the level of dieback using the different factors that can alter tree fitness (Archambeau et al. 2019; Lu et al. 2019). Using this approach for spatial vulnerability assessment over broad areas remains uncertain. Although many predisposing factors are often easily available, inciting or contributing factors are scarcely available, so that predictive performances may be poor. Here we evaluated if easily available geographic information describing climate variability and evolution, and the main soil and topographic characteristics, can be combined with remote sensing images to efficiently discriminate landscape-level canopy mortality patterns at a regional scale. The challenge consists in identifying and characterising the different factors correlated with the risk of dieback, determining which of them can benefit from adaptive management to mitigate the risk, and determining whether existing maps that describe their geographic distribution can be efficient to calculate a relevant vulnerability map.

Materials and Methods

Focusing on two emblematic stand types of European mountain ranges – silver fir and Norway spruce – we modelled the tree health status and mapped tree vulnerability across an 8,900 km² area located in the Vosges mountains, in northeastern France. For each species, a dataset was built with randomised plots selected on a systematic grid, and stratified according the stand status (dieback or healthy) collected from sentinel-2 images in 2019 (Fig.1). To identify the conditions that promoted decline, the plots were characterised with variables describing the site conditions (climate and soil characteristics, climate evolution) available from Geographic Information System (GIS) layers, and the stand characteristics interpreted from aerial photographs. Based on these datasets, models were calibrated and a vulnerability map was calculated at 50 m resolution for each species. The map performances were evaluated against ground survey data providing the volumes of dead wood harvested from exceptional sanitary cuts.

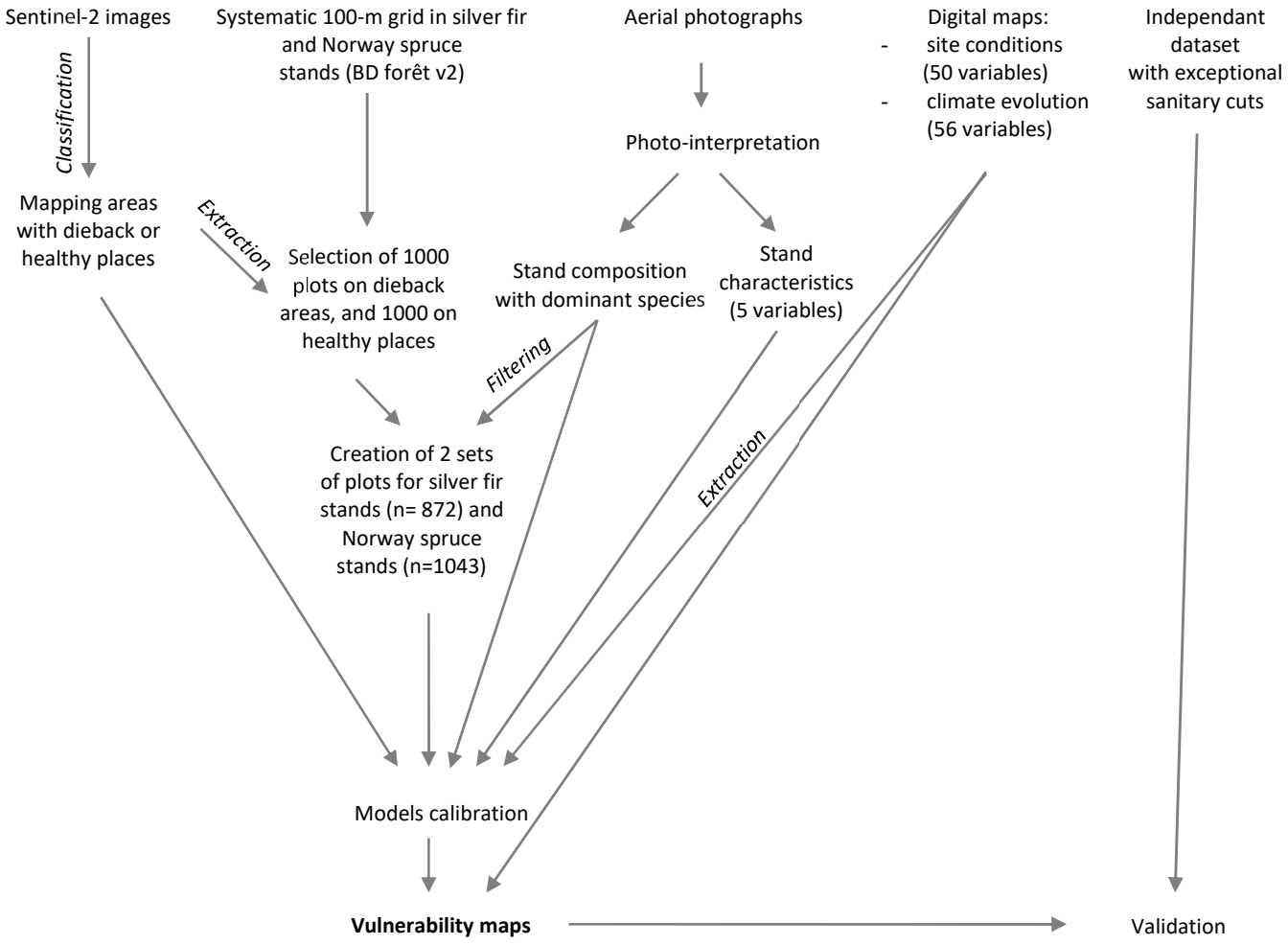

Fig. 1*: Workflow illustrating the different steps leading to the construction of the vulnerability map.*

Study area

The Vosges mountain range has contrasting soil and climate conditions. Altitude ranges between 200 m in the eastern plains of Alsace to 1,424 m at the "Grand Ballon" (Fig. 2A). Rainfall varies between 500 and 2,000 mm, and mean annual temperatures between 6°C and 11°C for the 1981-2010 period (Aurelhy model, Météo France). Geology mainly consists of acidic sandstones in the north and west of the study area, and magmatic rocks in the centre of the mountain range (Fig. 2B). Forests cover more than 60% of the territory, and provide important

economic and social benefits. In the national forest inventory plots[2], the most common productive tree species in the Vosges mountains are (in order of decreasing frequency): European beech (present in 75% of the plots), silver fir (59%), Norway spruce (53%), sessile oak (40%) and Scot pine (25%). Softwoods represent 70% of the stands, while silver fir or Norway spruce are the dominant species in 40 % of them (IGN BD forêt v2[3], Fig 2C). These two species represent approximatively 50% of the annual timber harvested in the massif (500,000 m^3).

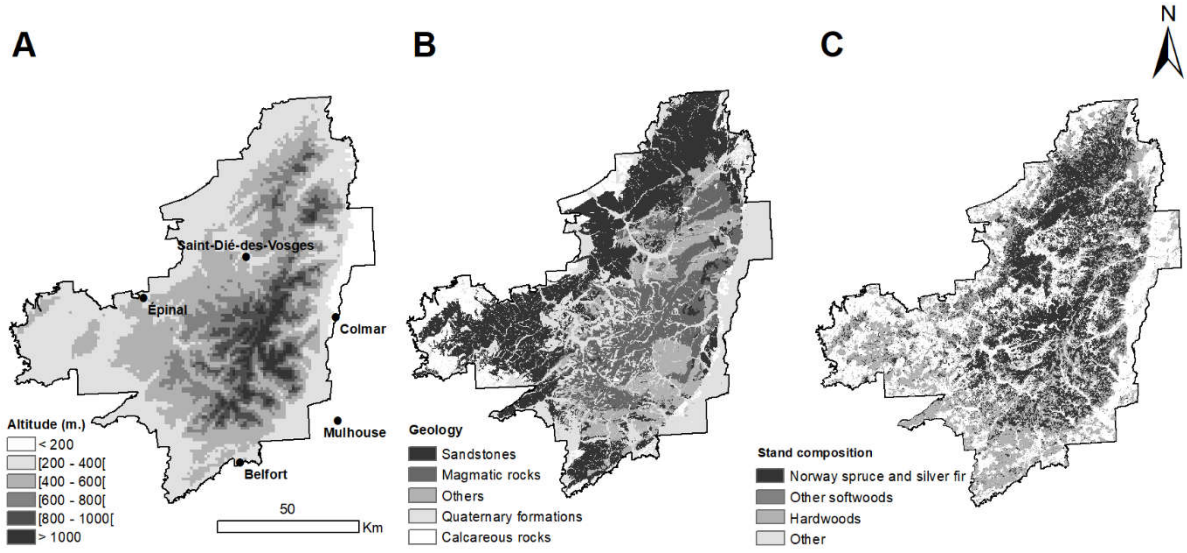

***Fig. 2**: Description of the study area: distribution of altitudes (A, IGN BD alti), simplified geology (B, BRGM geological map) and simplified stand composition (C, IGN BD forêt v2).*

Mapping of dieback using remote sensing data

We used three Sentinel-2 images level N2A downloaded from Theia website[4]. We selected images taken on July 24, 2019, during a period with little cloudiness and maximum vegetation cover to avoid confusion between the soil and dieback, and differentiate dead trees from living trees. These images were corrected for atmospheric, topographic and geometric effects. Dieback was identified through a supervised classification by excluding bare soil, crops, ground vegetation, urban areas, water, and forested areas. The classification was trained using 288 units presenting dieback, and validated with 1,814 others units including 285 units presenting dieback, collected

[2] https://inventaire-forestier.ign.fr/IMG/pdf/RF-Massif_vosgien.pdf
[3] https://inventaire-forestier.ign.fr/spip.php?article646

[4] https://theia.cnes.fr/atdistrib/rocket/#/search?collection=SENTINEL2

by photo-interpretation. The Sentinel-2 images were classified with ArcGIS Pro 2.5.0, using maximum likelihood classification (MLC, Sun et al. (2013)).

Sampling strategy

To avoid considering mortality patterns from other species than silver fir and Norway spruce, we used the IGN BD forêt v2[5] database to select vegetation units recorded on aerial photographs that showed these two species. A systematic 100-m grid was built, and 1,000 plots were randomly selected in dieback-struck areas and another 1,000 plots in healthy places.

We used aerial photos at 20 cm resolution to separate plots according to the dominant species (spruce or fir) and to identify the stand characteristics on 15-m-radius plots (seven classes, Table S1). We used photos dating back to 2018, taken prior to the dieback event, to identify the stand characteristics. To avoid the risk of confusion, only the classes where the studied species was dominant or not in mixture with the other studied species were kept for each dataset to avoid confusion (classes 1, 2, 3 and 5 in Table S1; 872 plots were selected for silver fir, and 1,043 plots for Norway spruce). For each plot, the stand's status (healthy or dieback) and 112 explanatory variables were collected in a database: 6 variables described the stand characteristics, 50 described the site conditions, and 56 described climate evolution.

Variables describing the stand characteristics

We collected six variables to describe the stand characteristics (Table1). We distinguished four levels of species mixture for stand composition (COMP, modalities 1, 2, 3 and 5, Table S1). For stand density (DENS) we differentiated dense stands from sparsely forested stands, where the ground was visible on more than 10% of the plot area. Age and structure effects (STRUCT) were recorded in three classes: old even-aged forest stand, young even-aged forest stand, and heterogenous structure. We also identified the presence of edges due to interfaces between different land uses (TYP_EDGE: absence of an edge, edge between two forest stands of different heights, and with an open environment), and the presence of edges facing south (variable EDGE_S). These variables were

[5] https://inventaire-forestier.ign.fr/spip.php?article646

collected using aerial photographs, on 15-m-radius plots (similar to classical forest inventory plots in France), for COMP, DENS, and STRUCT, and on 50-m-radius plots for TYP_EDGE and EDGE_S to consider data around the plot that could influence the stand health. Finally, we added data about the 1999 windstorm damage that had a strong impact on the Vosges mountains forests by rejuvenating some forest stands (STORM). These IGN maps differentiated areas with less than 10% damage from those with 10 to 50% damage or more than 50% damage.

	Category	Variable	Description	Source
STAND DESCRIPTION	STAND	COMP **	Stand composition: 4 levels of mixture	2018 aerial photographs
		DENS **	Stand density	
		STRUCT **	Stand structure	
		TYP_EDGE **	Presence of edges in the plot	
		EDGE_S **	Presence of an edge southward	
		STORM **	Forest damaged by the 1999 storm	IGN
SITE CONDITIONS	GEOLOGY	GEOL**	Simplified geological map	BRGM
	TOPOGRAPHY	ALT *	Altitude (m)	50 m resolution digital elevation model (DEM)
		COS_ASP *	Cosine of aspect	
		SIN_ASP *	Sine of aspect	
		SLO*	Slope (°)	
		CONT*	Containment in a 1,500-m radius (m.)	
		CURV*	Shape of the topographical surface (1,500-m radius)	
		TOPO*	Relative distance between ridge and talweg (m.)	
		REL_ALT*	Relative altitude between ridge and talweg (m.)	
		CURV*	Shape of the topographical surface (1,500-m radius)	
	SOIL NUTRITION	PH*	Bioindicated soil surface pH	(Gegout et al. 2003)
		CN*	Bioindicated soil surface C/N	
	SOIL WATER-LOGGING	TW*	Bioindicated temporary waterlogging	
		PW*	Bioindicated permanent waterlogging	
	ENERGY	RAD (wi, sp, su, an)	Solar radiation (2009-2019 period, J/cm²)	(Piedallu and Gegout 2007)
		TMIN (wi, sp)	Minimum temperature (2009-2019 period, °C)	(Piedallu et al. 2016)
		TMEAN (wi, sp, su, au, an)	Mean temperature (2009-2019 period, °C)	
		TMAX (su)	Maximum temperature (2009-2019 period, °C)	
	CLIMATIC WATER CONTENT	RAIN (wi, sp, su, au, an)	Cumulated rainfall (2009-2019 period, mm)	
		CWB (wi, sp, su, au, an)	Climatic water balance (2009-2019 period)	
	SOIL WATER CONTENT	DEPTH	Soil depth	(Piedallu et al. 2011)
		SWHC	Soil water holding capacity (mm)	
		SWC (sp, su, au, an)	Soil water content (Thornthwaite formula, 2009-2019 period)	(Piedallu et al. 2013; Thornthwaite and Mather 1955)
		SWD (sp, su, au, an)	Soil water deficit (PET-AET, 2009-2019 period)	
	SOIL WATER FLUXES	Kh	Horizontal hydraulic conductivity at saturation (m *per* day)	(Ondo et al. 2017)
		Kv	Vertical hydraulic conductivity (m *per* day)	
		FLUX (su, an)	Lateral surface and subsurface fluxes (mm)	
CLIMATE EVOLUTION	CLIMATE ANOMALIES	evTMIN (wi, sp)	Evolution of minimum temperature (°C)	
		evTMEAN (wi, sp, su, au, an)	Evolution of mean temperature (°C)	
		evTMAX (su)	Evolution of maximum temperature (°C)	
		evRAIN (wi, sp, su, au, an)	Evolution of rainfall (mm)	
		evCWB (wi, sp, su, au, an)	Evolution of CWB (mm)	
		evSWC (wi, sp, su, au, an)	Evolution of SWC (mm)	
		evSWD (wi, sp, su, au, an)	Evolution of SWD (mm)	
	CLIMATE TRENDS	regTMIN (wi, sp)	Minimum temperature trend	
		regTMEAN (wi, sp, su, au, an)	Mean temperature trend	
		regTMAX (su)	Maximum temperature trend	
		regRAIN (wi, sp, su, au, an)	Rainfall trend	
		regCWB (wi, sp, su, au, an)	CWB trend	
		regSWC (wi, sp, su, au, an)	SWC trend	
		regSWD (wi, sp, su, au, an)	SWD trend	

*Table 1: List of the 113 explanatory variables. All climate data were averaged over the 2009-2019 period, climate anomalies were differences between the 2009-2019 and 1961-1985 periods, and climate trends were the coefficients of regression calculated over the 1986-2019 period. wi = winter, sp = spring, su = summer, au = autumn, an = annual values. * monotonic and quadratic responses were evaluated, ** qualitative variables.*

Variables describing the site conditions

Fifty variables described the site conditions. They concerned geology (n=1), topography (n=9), soil nutrition (n=2), waterlogging (n=2), energy for plants (n=12) and water availability (n=24) (Table 1). A simplified geological map (GEOL) was drawn by merging similar substrates on the local maps at 1:50,000 scale elaborated by the BRGM. Topographical indices were calculated with the IGN 50-m digital elevation model for altitude (ALT), aspect – cosine of aspect (COS_ASP), sine of aspect (SIN_ASP), and slope (SLO). Topographical position was represented by four indices: containment (CONT), the difference of altitude between the pixel and the average altitude within a 1,500-m radius, curvature (CURV) that describes the shape of the topographical surface in the direction of the maximum slope within a 1,500-m radius (convex, flat or concave), and the relative distance (TOPO) and altitude (REL_ALT) of the cell along the toposequence (the ratio of the distance or altitude between the cell and the nearest ridge to the total length or the difference of altitude found in the toposequence), respectively. We characterised soil nutrition and waterlogging according to 1-km resolution maps built using bioindication techniques (Gegout et al. 1998) for soil surface pH, nitrogen nutrition estimated from the C/N ratio (CN), temporary waterlogging (TW) and permanent waterlogging (PW).

GIS layers of monthly climate variables were used to estimate energy and water available for plants over the 2009-2019 period (Table 1). Solar radiation (RAD) was calculated at 50 m resolution using Helios model (Piedallu and Gegout 2007). Monthly minimum, average and maximum temperatures and rainfall (TMIN, TMEAN, TMAX, and RAIN, respectively), were modelled and mapped at 1 km resolution (Piedallu et al. 2016). Climatic water balance (CWB) is the difference between rainfall and potential evapotranspiration according to Turc's formula (Turc 1961). One-km resolution maps of soil depth (DEPTH) and soil water holding capacity (SWHC) (Piedallu et al. 2011) were used to evaluate the soil water content (SWC, available water in the soil) and

234 the soil water deficit (SWD, the difference between potential evapotranspiration and actual evapotranspiration)
235 according to Thornthwaite formula (Thornthwaite and Mather 1955). In addition, three indices characterising
236 lateral fluxes in the soil were extracted from GIS layers. Kh and Kv represented the horizontal and vertical
237 hydraulic conductivity at soil saturation, respectively, and FLUX estimated the balance between the input and
238 output surface and subsurface fluxes (Ondo et al. 2017).

239

240 All the variables including climate were averaged over the ten years before data collection (2009-1019),
241 *per* season (winter -wi, December to February-; spring -sp, March to May-; summer -su, June to August; and
242 autumn -au, September to November), and over the whole year (an).

243

244 ## Variables describing climate evolution

245 Two sets of calculations – climate anomalies and climate trends – were used for temperatures (TMIN,
246 TMEAN, TMAX), and water availability (RAIN, CWB, SWC and SWD, Table 1). Climate anomalies represented
247 the evolution between a reference period and a contemporary period. A period of ten years before data collection
248 (2009-2019) was selected to represent the contemporary period because tree death can be triggered by the
249 cumulative effects of many disturbances (Das et al. 2013). We selected 1961-1985 as the reference period because
250 significant warming occurred in France after 1986 (Taccoen et al. 2019).

251

252 Climate trends were calculated for the same variables over the 1986-2019 period. For each variable and
253 each pixel of 1-km resolution, the trends were regressed against time for the 32 studied years, and the linear
254 regression coefficients were mapped. A positive slope indicated an increase of the climatic constraint for TMIN,
255 TMEAN, TMAX and SWD, and a decrease for RAIN, CWB and SWC.

256

257 ## Modelling approach and vulnerability map calculation

258 We modelled silver fir and Norway spruce mortality with logistic regression (McCullagh and Nelder
259 1997). For each species, we evaluated the 113 explanatory variables through a forward stepwise procedure. At

each step, the variable explaining the maximum deviance was selected if it was statistically significant ($P < 0.01$), and little correlated with the previously selected variables (Pearson's $r < 0.7$). Because monotonic responses were expected, quadratic responses were not considered for the climate variables. However, monotonic and quadratic response curves were both evaluated for the other variables. The process ended when the selection of a new variable led to a d^2 increase lower than 0.01 or a p-value > 0.01.

The receiver operating characteristic (ROC) curve was calculated to evaluate the performances (Fielding and Bell 1997), and different metrics were used: the area under the ROC curve (AUC), the kappa index, success (the rate of good prediction), sensitivity (the rate of good prediction of presence), and specificity (the rate of good prediction of absence) (Manel et al. 2001). The relative importance was calculated for each variable using the drop contribution (Lehmann et al. 2002), *i.e.,* the difference in explained deviance between the full model and a partial model when the variable was dropped. The ratio of the drop contribution of the variable over the sum of the drop contributions for all the variables gave the relative importance of each predictor.

The ROC curve also provided the optimal threshold for predicting the presence / absence of dieback. It was used to calculate the vulnerability map: upper values delineated the "high level of vulnerability" class where the stands were predicted dead by the model, while lower values were divided in three classes with equal intervals of increasing vulnerability. The map was calculated using the GIS layers describing the environmental predictors selected in the model. The best resolution among the selected variables was kept (i.e. 50 m). The vector layers were rasterised, and the 1km resolution maps were resampled using the bilinear interpolation algorithm. The map included four levels of vulnerability, calculated from a type stand used across the whole area.

Validation dataset

A map of the volumes of harvested dead wood from exceptional sanitary cuts was provided by the ONF for public forests, which cover 2/3 of the forested area of the Vosges mountains. We selected areas where one of the studied species was dominant or not in mixture with the other studied species. For 7,355 management units identified for silver fir (11,218 for Norway spruce), the average volume of dead wood was compared for the different vulnerability levels. Our vulnerability maps were drawn using 2019 satellite imagery, but dieback may

have occurred before or after this date in the most vulnerable areas. As a consequence, we considered both the volumes of dead trees recorded in 2019 and the sum of the volumes over the 2018-2020 period.

Results

Distribution of silver fir and Norway spruce dieback in the Vosges mountains

The classification of sentinel-2 data predicted 92% of the stand status of the validation dataset correctly. It identified 2,072 ha of dieback in the Vosges mountains, representing 1.4% of the studied stands. We observed dieback on 362 plots out of the 872 plots selected for silver fir, and on 627 plots out of the 1,043 plots selected for Norway spruce, mainly in the south and the north of the studied area (Fig. 3). Eighty-five plots were deleted due to the risk of confusion because the two species were in mixture and neither was dominant, or the stands were too young and the species were impossible to identify. The selected plots were distributed across the whole studied area: the average distances to the nearest plot were 1,015 and 932 m for silver fir and Norway spruce, respectively. These distances increased up to 1,105 and 1,356 m in the dieback stands, even though they were oversampled.

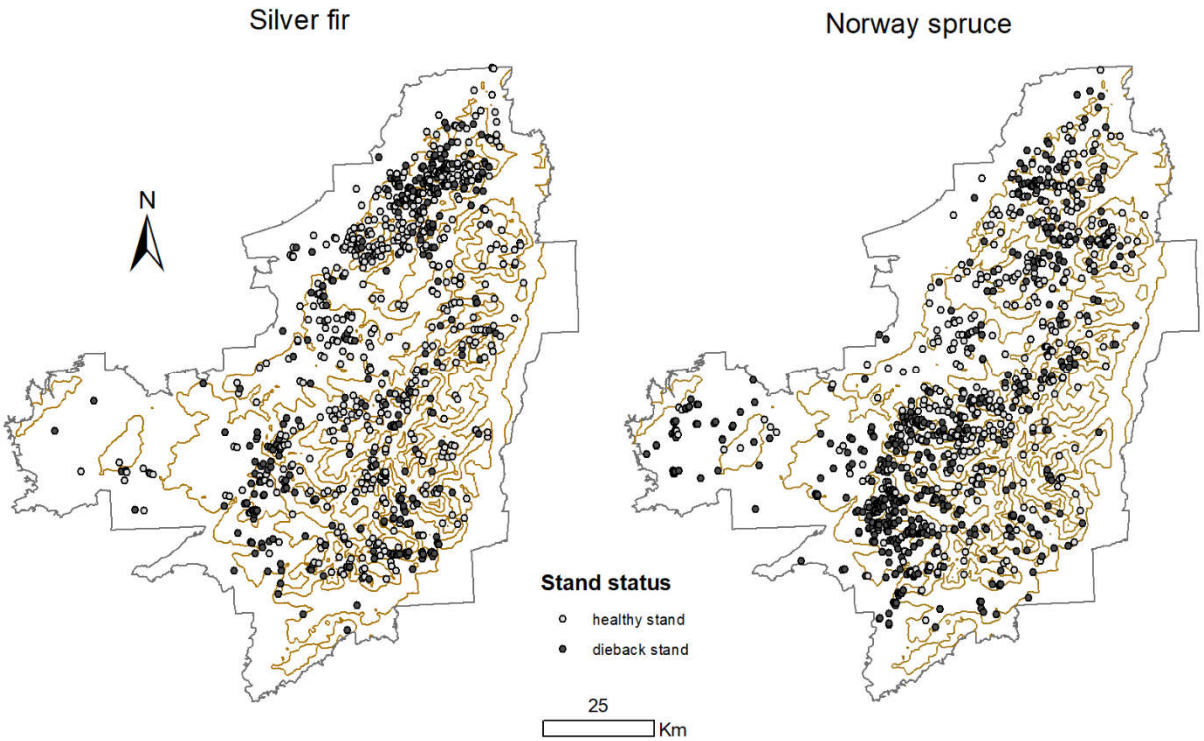

303 ***Fig. 3**: Localisation of the stands with dieback symptoms for silver fir (n= 872) and Norway*
304 *spruce (n= 1,043) in the Vosges mountains.*

305

306 **Silver fir and Norway spruce dieback modelling**

307 With respective AUCs of 0.80 and 0.78 and nine variables selected, the silver fir and Norway spruce
308 dieback models showed similar performances and near predictors (Figures 4 and 5). They combined variables
309 describing stand composition and structure, local conditions and climate evolution to various extents according to
310 the species (Figure S1). Environmental conditions explained 59% of the deviance for silver fir *versus* 62% for
311 Norway spruce. Geology and stand composition were among the most important variables correlated with dieback
312 for both species, in addition to the presence of an edge southward for silver fir and temporary waterlogging for
313 Norway spruce. The trend in summer soil water deficit was directly linked to climate change (relative importance
314 ranging between 6 and 7%).

315 Less dieback occurred for both species when they were in mixture in stands dominated by broadleaved
316 species. Mortality was significantly higher in pure stands for Norway spruce (Fig. 4 and 5). More dieback was also
317 identified in even-aged stands compared to uneven-aged or young stands when a forest edge was present (with a
318 clear effect of a south forest edge for silver fir), and in stands that underwent little damage during the 1999 storm.
319 Silver fir and Norway spruce mortality also responded to five environmental variables (Fig. 4 and 5). Silver fir
320 showed a higher risk of dieback when it grew on volcanic pyroclastic rocks, neutral to basic rocks, principal
321 conglomerate or acidic granite. Norway spruce showed lower substratum-dependent differences than silver fir did,
322 and was more prone to dieback on sedimentary basic rocks, Voltzia or shell sandstone. Both species were also
323 sensitive to topographical position, with a higher risk of dieback in areas near the ridges, on the south slopes, and
324 when waterlogging was present. Finally, increased dieback was observed with soil drying. High values
325 corresponded to a strong increase of the soil water deficit during the 1986-2019 period (Fig. 4 and 5, equations for
326 the two species can be found in Table S2 and S3).

327 The risk of dieback linked to environmental conditions and stand characteristics varied according to the
328 location for both species (Fig. 6, 7, B, C). The vulnerability maps[6] calculated at 50 m resolution (Fig. 6-D and 7-

[6] The vulnerability maps for silver fir and Norway spruce dieback can be downloaded from the SILVAE website (https://silvae.agroparistech.fr/home/)

329 D) identified 7% of the stands with a high level of vulnerability for silver fir *versus* 33 % for Norway spruce, while
330 83% of the stands were classified as presenting a low or very low level of vulnerability for silver fir *versus* 26 %
331 for Norway spruce (Fig. 8). In the validation dataset (Fig. 9), we observed a significantly higher volume of dead
332 trees for the class showing a high level of vulnerability than for the other classes. This difference was higher for
333 silver fir (about ten-fold) than for Norway spruce (about two-fold).

334

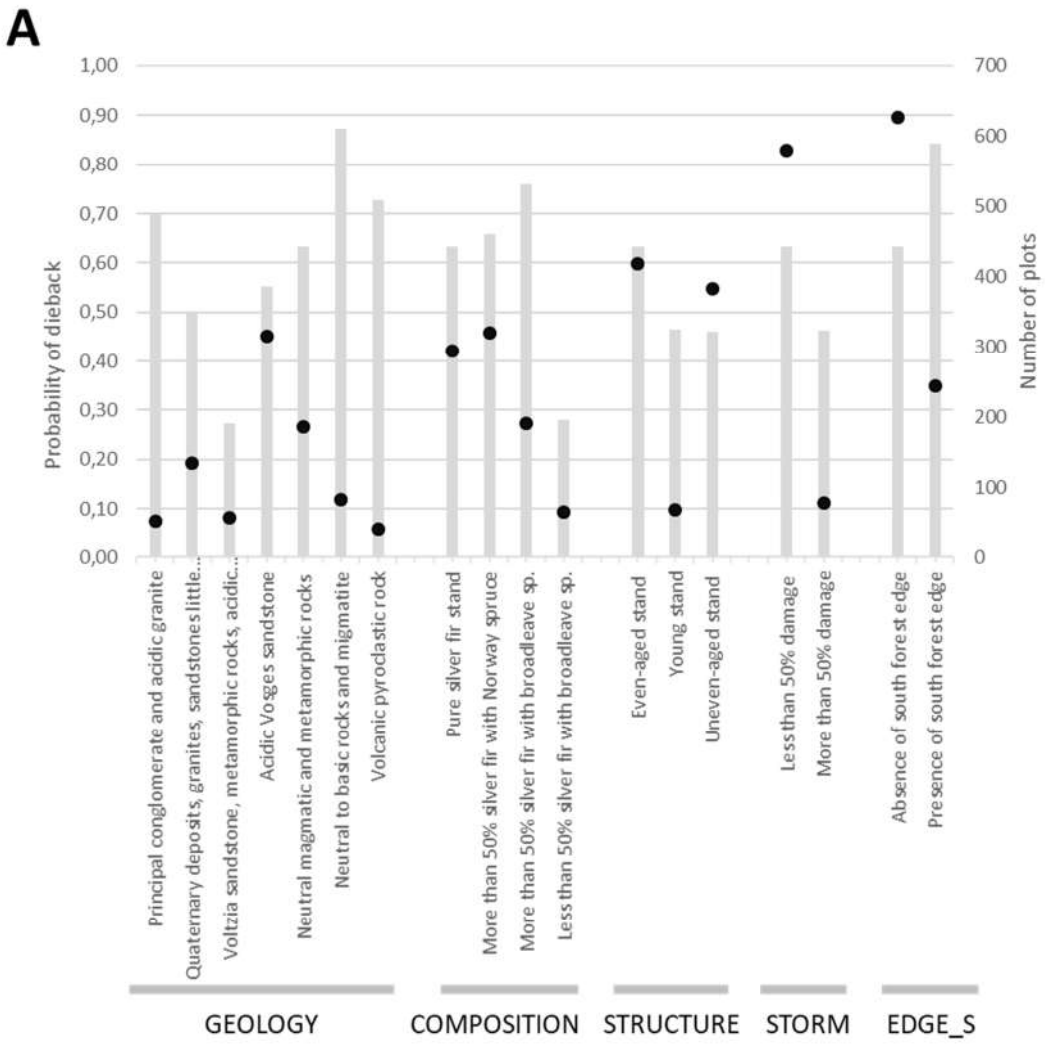

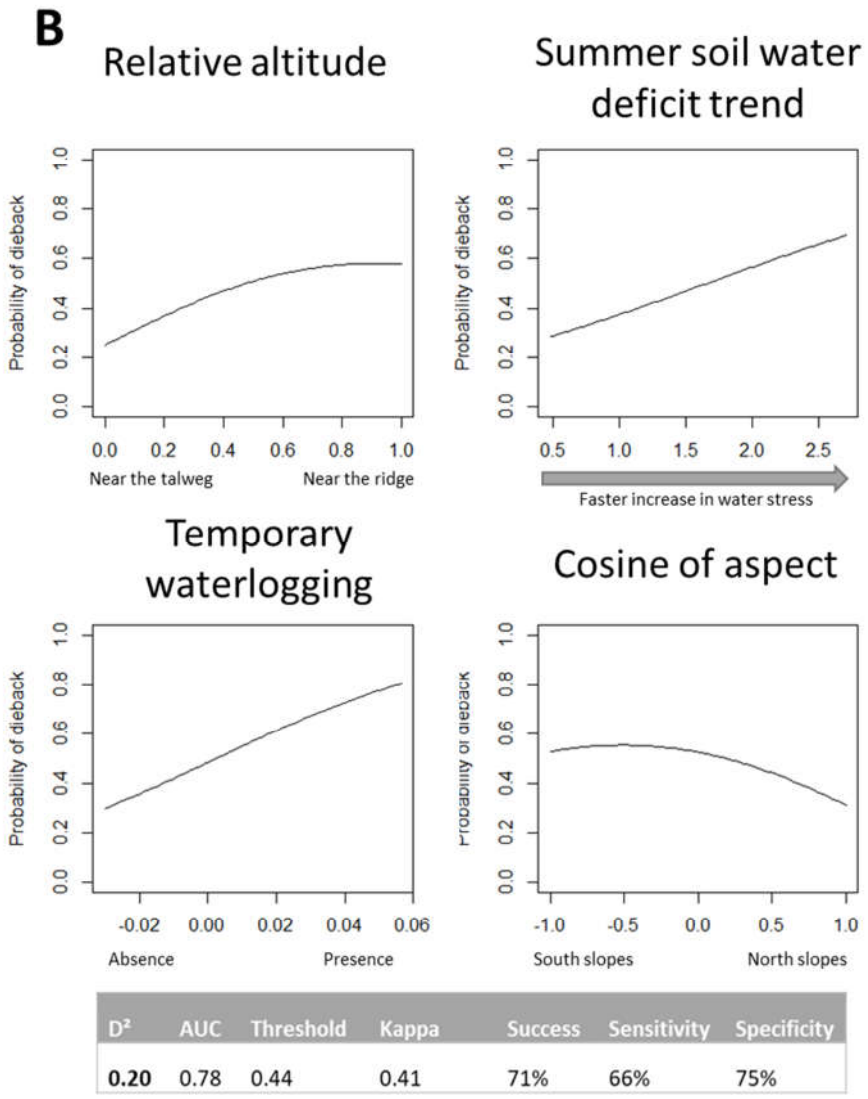

D^2	AUC	Threshold	Kappa	Success	Sensitivity	Specificity
0.20	0.78	0.44	0.41	71%	66%	75%

***Fig. 4**: Performances of the silver fir model and differences in the probability of dieback according to the variables (A: qualitative variables, B: quantitative variables). The response curves were calculated using mean values for the other quantitative variables, and the following modalities for the qualitative variables: GEOLOGY, "Neutral magmatic and metamorphic rocks", COMPOSITION: "Pure silver fir stand", STRUCTURE, "Even-aged stand", STORM: "Less than 50% damage during the 1999 storm". and EDGE_S (Presence of an edge southward), "Absence of a south forest edge". Black dots in fig. 4A: numbers of plots for each modality.*

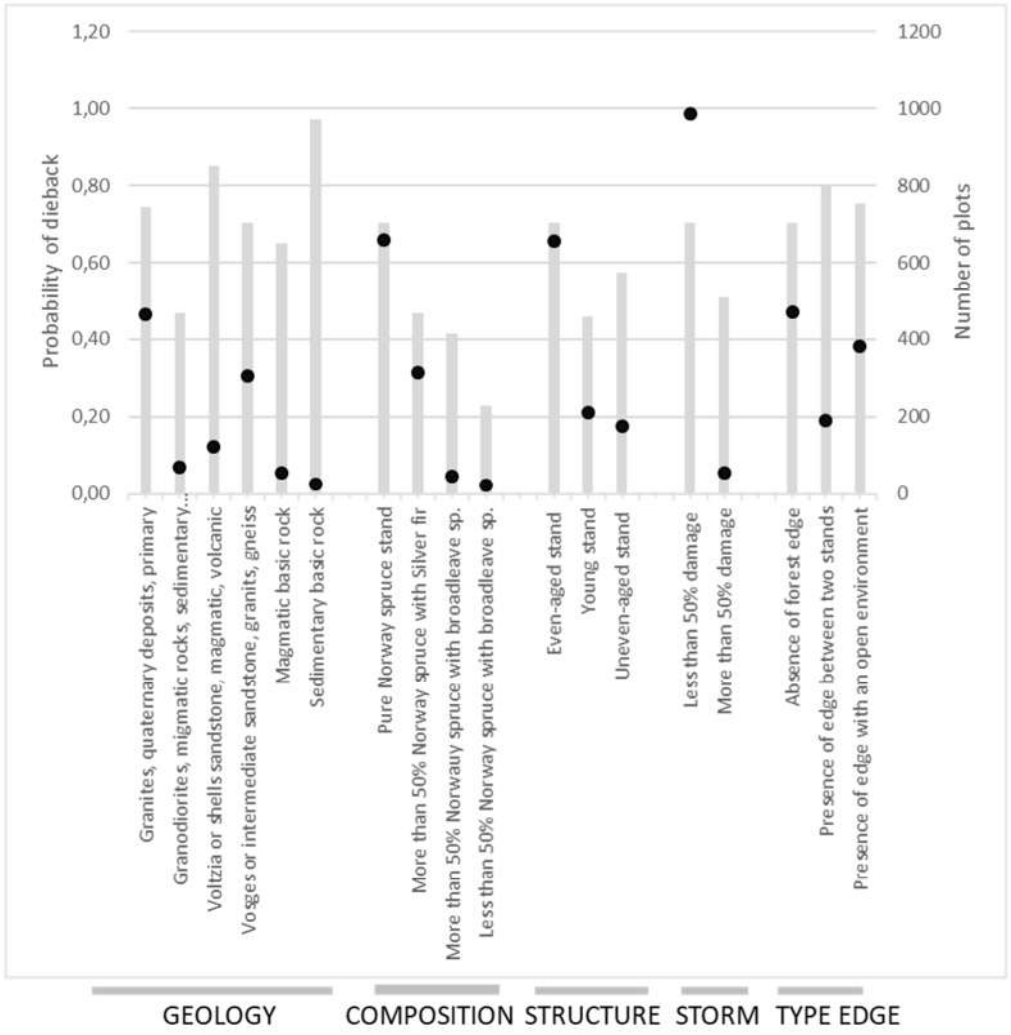

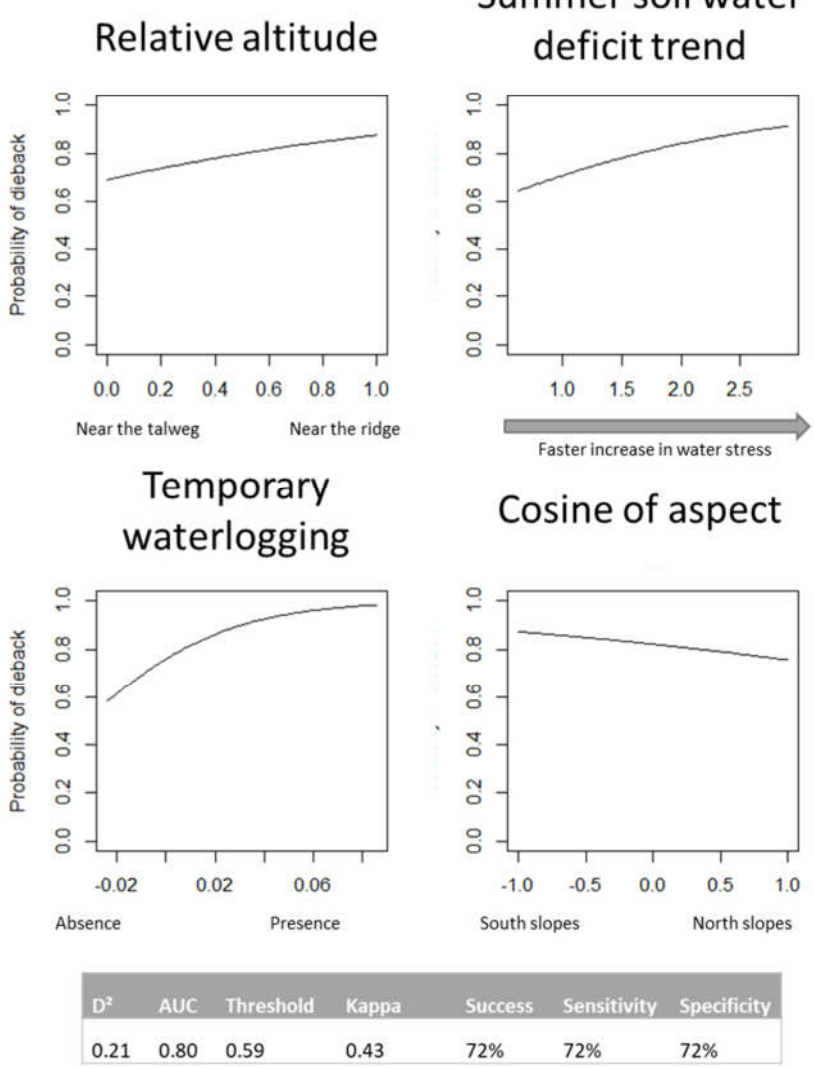

D^2	AUC	Threshold	Kappa	Success	Sensitivity	Specificity
0.21	0.80	0.59	0.43	72%	72%	72%

342

Fig. 5: *Performances of the Norway spruce model and differences in the probability of dieback according to the variables (A: qualitative variables, B: quantitative variables). The response curves were calculated using mean values for the other quantitative variables, and the following modalities for the qualitative variables: GEOLOGY, "Vosges or intermediate sandstone, granites, gneiss", COMPOSITION: "pure Norway spruce stand", STRUCTURE, "even-aged stand", STORM, "Less than 10% damage during the 1999 storm", and TYPE EDGE "Absence of a forest edge". Black dots in fig. 5A: numbers of plots for each modality.*

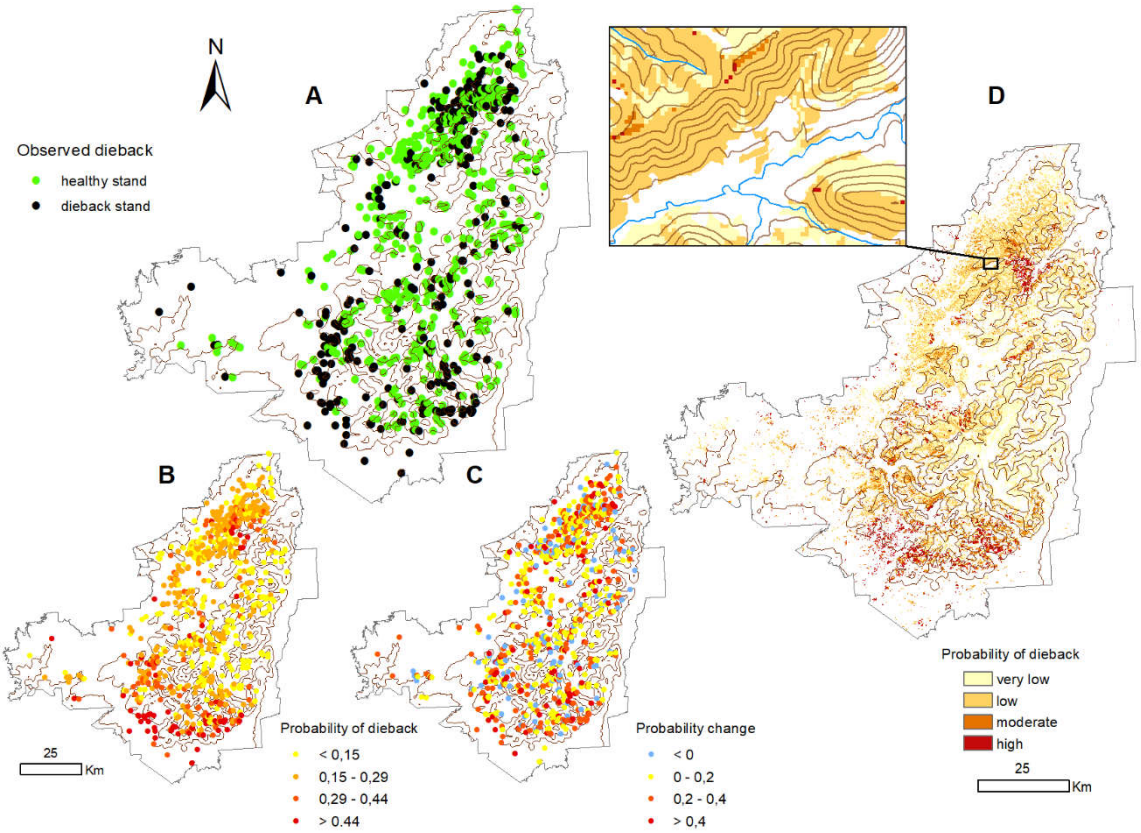

Fig. 6*: Silver fir dieback observed (A) or predicted in the sampled plots (B, C, n = 872), and vulnerability map (D). B: Dieback explained by environmental conditions only (variables GEOL, REL_ALT, regSWD_su, TW and COS_ASP). C: modulation of vulnerability predicted on map B due to the stand characteristics (variables COMP, STRUCT, EDGE_S and STORM). D: The vulnerability map was calculated with the modalities "Absence of a south forest edge", "Even-aged stand", "Pure silver fir stand" for the variables EDGE_S, STRUCT and COMP, respectively). The "high level of vulnerability" class corresponds to the values greater*

than the optimal threshold obtained from the ROC curve; lower values were divided in three classes of equal interval (the break values are used for the legend on map B).

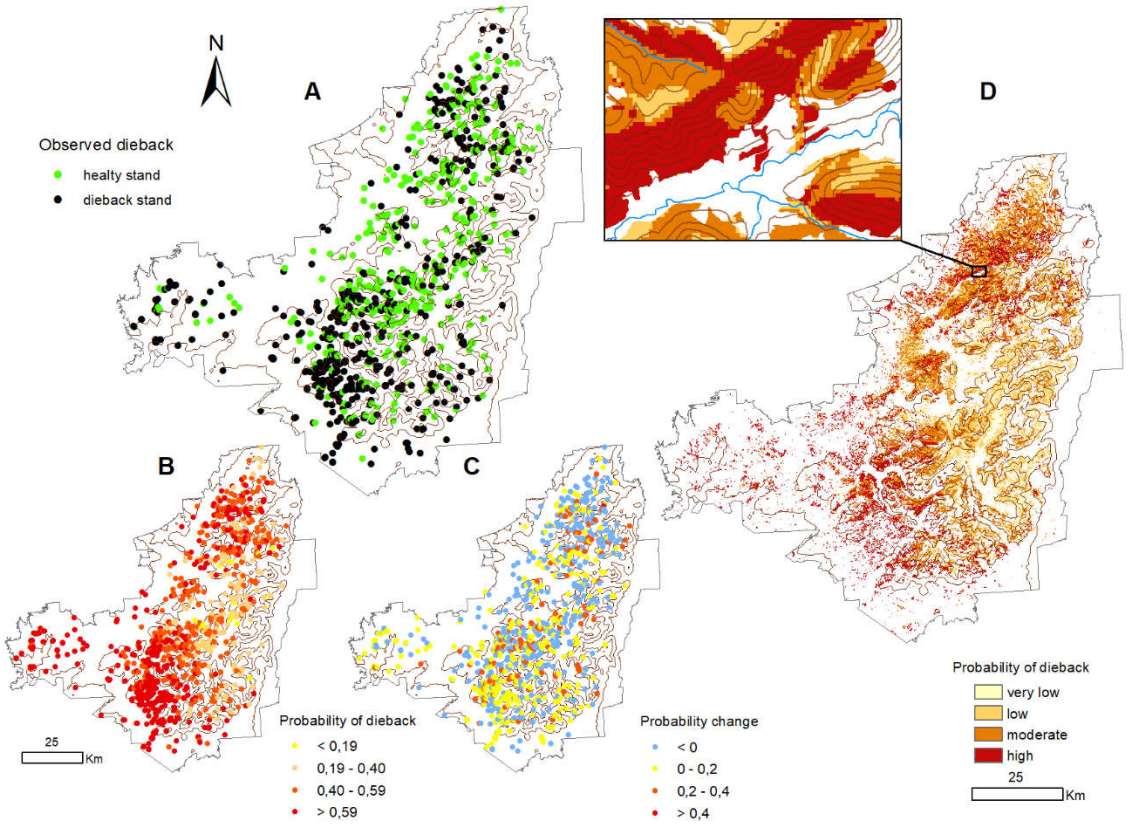

Fig. 7*: Norway spruce dieback observed (A) or predicted in the sampled plots (B, C, n = 1,043), and vulnerability map (D). B: Dieback explained by environmental conditions (variables GEOL, REL_ALT, regSWD_su, TW and COS_ASP). C: modulation of vulnerability predicted on map B due to the stand characteristics (variables COMP, STRUCT, STORM and TYP_EDGE). D: The vulnerability map was calculated with the modalities "pure Norway spruce stand", "even-aged stand", and "absence of a forest edge" for the variables COMP, STRUCT and TYP_EDGE, respectively. The "high level of vulnerability" class corresponds to the values greater than the optimal threshold from the ROC curve; lower values are divided in three classes of equal interval (the break values are used for the legend on map B).*

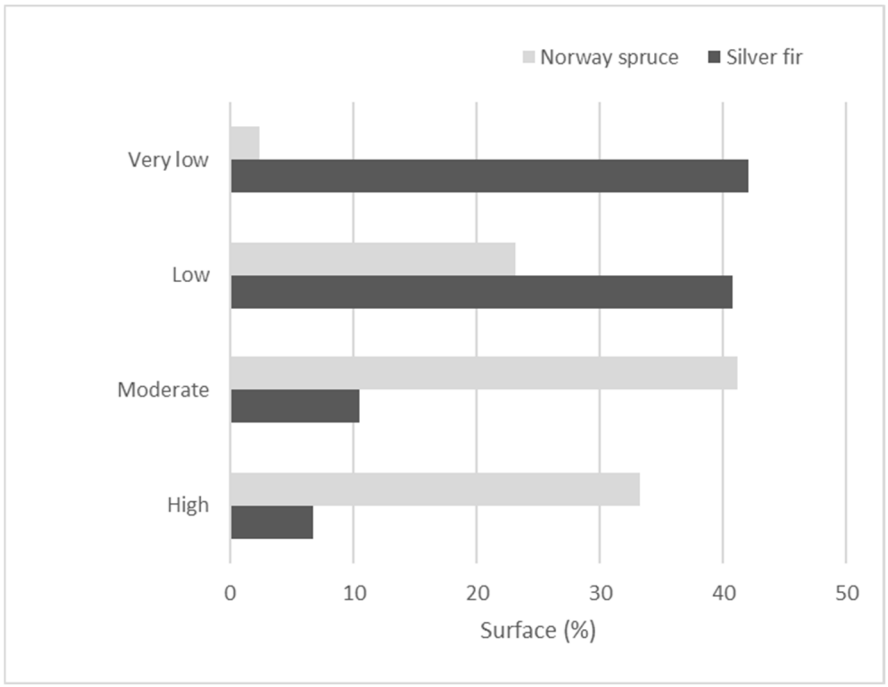

369

370 ***Fig. 8****: Distribution of the surfaces (%) with the different levels of vulnerability for the silver fir and Norway*

371 *spruce stands.*

372

373

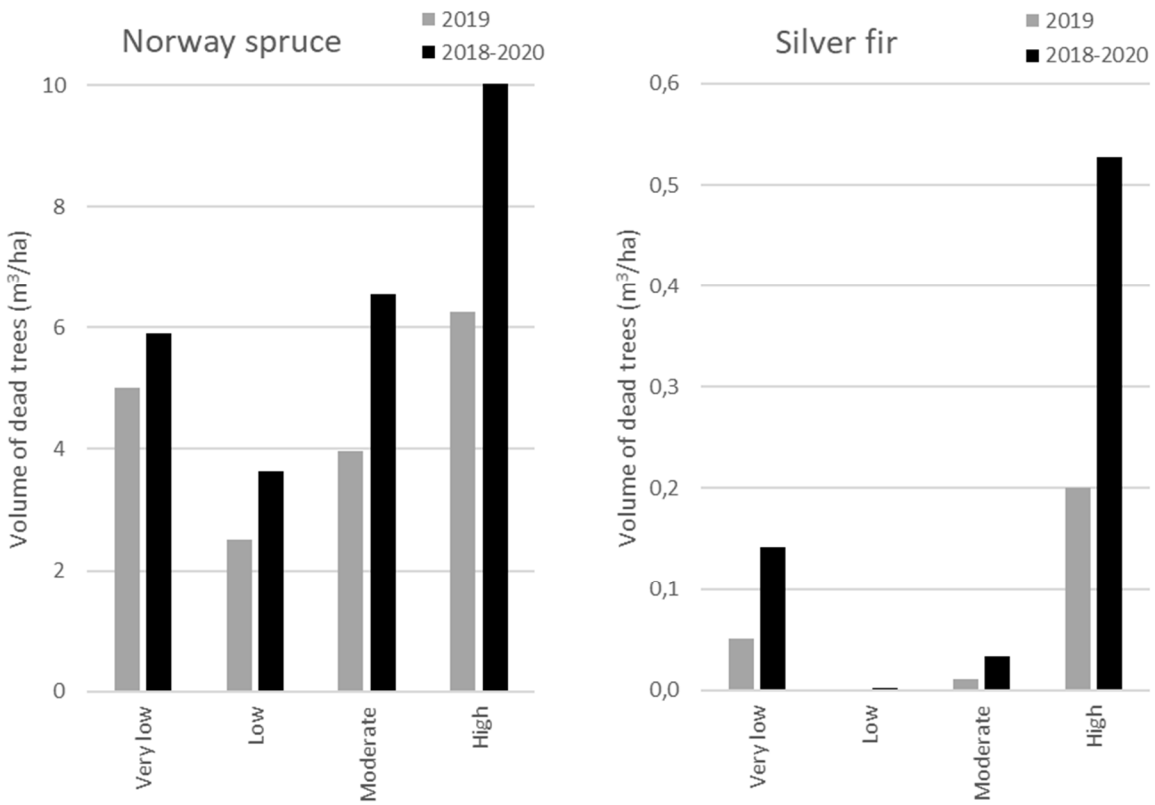

374

375 ***Fig. 9:*** *Volume of dead trees (m^3/ha) recorded in the silver fir and Norway spruce stands (ONF), according to*
376 *the four levels of vulnerability (trees inventoried in 2019 or between 2018 and 2020).*

377

378

379 # Discussion

380

381 ## A relevant method for large-scale spatial vulnerability assessment

382

383 Tree species vulnerability is an issue of growing concern round the world, but it is not new in managed
384 forests. After the 1911 drought in the centre and west of France, Roulleau already reported, "I see everywhere
385 […], in the cooler parts like the drier ones, a lot of trees are dying […] I have long recommended caution in the
386 use of Norway spruce" (Roulleau 1912). These observations concerned lowland areas, where the species was

387 introduced outside of its natural range. Conditions are different in the Vosges mountains, that benefit from colder
388 and wetter conditions typical of middle mountains of European climate. In this area, silver fir is a native,
389 emblematic species, while Norway spruce is considered as natural near the top of the mountain range (Guinier
390 1959). Yet, we found large surfaces threatened by forest decline (ranging between 7% for silver fir and 33% for
391 Norway spruce). In agreement with observations in Germany (Maringer et al. 2021), we observed a higher
392 vulnerability of Norway spruce than of silver fir.

393

394 The levels of vulnerability estimated on the map successfully discriminated the volumes of dead trees
395 recorded in public forests, highlighting the benefit of using easily available geographic information for the spatial
396 vulnerability assessment of silver fir and Norway spruce dieback. Despite less precision compared to traditional
397 ground surveys, the use of satellite imagery, photointerpretation and digital maps of environmental factors allowed
398 us to sample a large number of plots distributed along large environmental gradients. As far as the mapping results
399 are concerned, the better performance of silver fir compared to Norway spruce can be explained by the large extent
400 of Norway spruce dieback across a wide variety of ecological conditions, and its higher susceptibility to bark beetle
401 attacks (de Groot and Ogris 2019). Existing vulnerability assessment was mostly based on mortality observed the
402 previous years (Preisler et al. 2017), changes in tree fitness visible by satellite imagery (Verbesselt et al. 2009), or
403 the identification of weakened trees with declining growth (Suarez et al. 2004). We propose a method based on
404 easily available geographic information, that can be implemented over broad areas, to monitor dieback of different
405 species and over different periods of time. When data is available, it can be coupled with forest inventory
406 information for a better description of the stand characteristics.

407

408 The selected variables were linked to stand characteristics, geology, and water availability, with a clear
409 effect of climate change. Large differences were highlighted relatively to the latest important tree decline event
410 experienced in Europe during the 1973-1981 period. At that time, more mortality was observed for old trees located
411 at low or high altitudes, on acidic substratum, and in the east of the mountain range (Bonneau 1985; Thomas et al.
412 2002). We are now observing lower mortality at high altitude, no more mortality on acidic substratum compared
413 to the other areas, and a greater decline in the south and the north of the mountain range. These differences suggest
414 that dieback is currently triggered by different factors than those identified during the 1980s.

415

Importance of water availability in silver fir and Norway spruce dieback

Dieback of both silver fir and Norway spruce responded markedly to water balance variables in our models. The soil water deficit trends performed better than climate anomalies or variables describing average climate. This result stresses the importance of the dynamic of soil water availability in dieback evaluation. The effects of drought on tree decline have been largely studied, but most of the large-scale studies tried to relate forest dieback to average climate conditions over long periods (Lu et al. 2019). For a given current soil water deficit, we observed that impacts on trees were greater when the deficit had sharply increased in the last years compared to areas under recurring deficit (Figure S2). These outcomes suggest that a tree of a given species can be more resilient to drought when it has grown in drier conditions, as observed by Gazol (2017) both in the north of America and Europe. They also highlight that the dynamic of water stress over time should be considered rather than average climate to forecast mortality patterns. Our understanding of the time span that should be investigated to efficiently evaluate stand vulnerability should also be improved.

Several other selected variables were related to water availability. The higher risk of dieback observed near the ridges was related to the lateral redistribution of the soil moisture along a topographical hillslope gradient (Ondo et al. 2017). Some authors reported 15 to 90% lower soil moisture near the crests compared to the valleys (Western et al. 2004). The more severe dieback symptoms on south slopes can be attributed to their higher evaporation and transpiration, and differences in thawing. Rouse et al. (Rouse and Wilson 1969) observed 50% more water stored in the north slope soils than in the south slope soils in early spring. The increasing mortality with temporary waterlogging intensity can be interpreted in different manners. Both silver fir and Norway spruce avoid compact or waterlogged soils. Waterlogging also influences the plant water uptake by affecting the spatial distribution of fine root growth and limiting their depth (Fujita et al. 2021). Finally, the presence of edges (particularly south edges for silver fir), stresses the importance of microclimatic conditions. Increased temperature, light, and wind speed that increased evapotranspiration and decreased the soil water content have been recorded from 40-50 m from the edge (Chen et al. 1995), leading to higher tree mortality rates (Mesquita et al. 1999). These predictors related to the water balance represented 51% and 48% of the explained model deviance for silver fir and Norway spruce, respectively. They all showed an increase of dieback when the water balance components shifted toward less available water for trees.

Stand characteristics complement environmental predictors to explain dieback

Although stand data were collected by photo-interpretation – a less accurate method than field inventories – we demonstrated that stand characteristics could also explain dieback, with similar responses of the two studied species. We observed less mortality for uneven-aged stands and mixtures. These results are in agreement with previous studies showing lower resistance to disease and damage in even-aged stands than in uneven-aged stands (Pukkala et al. 2013). The negative effect of pure stands supports the results of previous studies demonstrating the benefits of functional diversity on tree resilience (Gazol and Camarero 2016), which can be explained by facilitation and resource partitioning. Facilitation is an interaction between species that benefits to at least one of them, while resource partitioning refers to the way different species can share resources over time or across space (Mc Cook 1994). Lower Norway spruce dieback was shown in stands dominated by beech (Pretzsch et al. 2020), attributed to complementarity in water uptake. A temporal shift between the two species provided Norway spruce better resistance to drought events (Rotzer et al. 2017). These effects are greater in low-productivity sites, as already observed in the Vosges mountains (Lebourgeois et al. 2013).

We also found less dieback in young stands or stands that had suffered important damage during the 1999 storm. The lower mortality of small trees compared to large ones could be attributed to differences in fine root distribution, in vulnerability to biotic factors, and to the greater water uptake difficulties of tall, large trees (Pfeifer et al. 2011). Because silver fir and Norway spruce dieback increase with basal area (Taccoen et al. 2019), this lower mortality could also be linked to limited competition for light or water in young stands. Lowering the basal area is often considered as a silvicultural tool to decrease tree vulnerability to drought and improve productivity (Pretzsch 2005). In agreement with studies demonstrating the strongest negative growth trends in pure and even-aged productive forests of conifers (Ols and Bontemps 2021), we suggest to promote an evolution of silvicultural practices toward mixed stands of uneven-aged trees to limit the stand basal area and avoid brutal cuts to limit edge effects (that can also reduce wind damage). The cumulated effect of these measures would lead to a significant decrease of the dieback vulnerability for the two studied species.

Using the map to mitigate the effects of climate change on silver fir and Norway spruce forests

The map makes it possible to prioritise the level of vulnerability for each studied species in view of helping forest managers to mitigate the effects of climate change. It can help to adapt the stands by forward planning, by guiding forest policies and silvicultural practices and helping to select suitable species or provenances. The map can be used directly because it instantly provides an evaluation of the vulnerability based on environmental conditions according to the geographic location. When basic information about stand structure and composition can be surveyed (using ground surveys or aerial photographs), the prediction can be improved: the effects of the stand characteristics can be evaluated, and the map gives information about the potential decreasing vulnerability if the stand characteristics allow for better tree resilience.

The future of Norway spruce and silver fir is probably strongly compromised in the most vulnerable areas identified by a high level of vulnerability on the map. These two species should be monitored in these areas on a priority basis, e.g., by raising the rate of transparency of the crown in some representative plots, or by using NDVI indices based on remote sensing data (Rogers Brendan et al. 2018). They should be preferentially cut when the first signs of degradation appear, and should not be replanted afterwards. Reforestation should rely on adequate forest regeneration promoting drought-tolerant species if available. Species more resistant to drought could also be introduced by selecting species that are visually close to those they replace in areas of high landscape interest. When the level of vulnerability is low or moderate, the strategy can be to promote a rapid evolution of silvicultural practices to adapt stand structure and composition in priority. The aim is to mitigate the effects of climate change in areas that can become highly vulnerable in the next decades. The areas with the lowest level of vulnerability would not be a priority in the first place but should also be monitored. The vulnerability map should be updated at regular time intervals to take the evolution of the soil water deficit and observed mortality changes into account, and adjust recommendations accordingly.

Limitation and uncertainties

The risk of decline was predicted efficiently although inciting and contributing factors were not explicitly considered. We expected them to be indirectly and partly taken into account by the climate variables selected in the models. The trend of the soil water deficit variable was probably influenced by the extreme drought events and

linked to the distribution of pathogens, which is also influenced by climate – particularly temperature (Baier et al. 2007). This result was probably observed because bark beetle attacks – which are severe in the area – occur preferentially on weakened trees (Kolb et al. 2019). Data describing the dynamics of pathogen populations could probably successfully complement the variables selected in the model, but spatial data depicting their spatial distribution and evolution remains scarce (Jaime et al. 2019). The model performance could also probably be improved by including variables of extreme events and disturbances when available, e.g., wind conditions and storm frequency, drought intensity, forest fires (Carnicer et al. 2011), or air pollution (Pedersen 1998). In addition, different modelling techniques could be compared to evaluate if the map performance could be improved.

We chose a spatial approach aimed at linking spatial heterogeneity related to the site conditions and stand characteristics on the one hand with the regional patterns of dieback on the other hand. We probably under-estimated the surfaces concerned by dieback because isolated dead trees or low symptoms were probably not identified by remote sensing approaches, and the dead trees in some of the dead stands were probably felled by forest managers before the satellite images were taken. This probably decreased the model performances, but with a limited influence on the estimation of vulnerable areas, as cuts probably concern a wide variety of ecological and stand conditions. This approach should be complemented by a temporal follow-up of the dieback dynamic using time series images and requiring inventories at different periods, to better identify recent cuts of dead trees, take the effect of extreme events into account, and simulate probabilities of dieback according to future climate conditions (Knight et al. 2013; Staupendahl and Zucchini 2011).

According to the classification of sentinel-2 images, dieback observed at a specific date is a relatively rare statistical event. To overcome this limitation, the proportion of areas with dieback was oversampled by selecting 50% of plots in dieback areas to calibrate the models. This method yielded correct regression coefficients, but it increased the intercept value, so that the probability of dieback in the model outputs was overestimated (King and Zeng 2001). Therefore, the probability of dieback provided by our model should not be interpreted as real probabilities, but it makes it possible to compare the effects of the qualitative variables and to interpret the shape of the response curve for the quantitative ones. This oversampling effect was corrected for the vulnerability map by using the ROC curve, which determines the classes of increasing levels of vulnerability according to the optimal

statistical threshold for each species. Despite a great average distance between each plot and its nearest neighbour, further analysis could also test for an effect of autocorrelation.

The resolution of the GIS layers describing the spatial variations of the environmental predictors also probably influenced the performance of the vulnerability map (Cavazzi et al. 2013). The variables selected in the models were at different spatial resolution: 50 m for relative altitude and the cosine of aspect, 1:50,000 map scale for geology, and 1 km resolution for temporary waterlogging and the trend in soil water deficit. We calculated the map at the finest spatial resolution (i.e., 50 m) to keep the contribution of local information available in the models. The other raster variables were resampled at 50 m resolution using the bilinear method, and geology was rasterised at 50 m resolution. It would also have been possible to aggregate the 50m resolution variables at 1km resolution. These different approaches could be compared to evaluate the effect of spatial resolution on the map performance. Dieback can vary at a very local scale, so we can reasonably believe that finer resolution predictors could improve the vulnerability map. Further work could also evaluate if the spatial resolution of the different predictors can be decreased with efficiency.

We demonstrated a good correlation between the different vulnerability levels and the ground survey quantifying the volumes of dead wood. However, the data or methods used in this study have their own limitations. Validating dieback data is a tricky task because it is difficult to collect independent and relevant datasets about dead trees, which are usually rapidly harvested and do not appear in forest inventory plots. In the studied area, this level of information is available about public forests through recordings of volumes of harvested dead wood from exceptional sanitary cuts. It was first collected for each management unit by different managers, and then aggregated at the massif scale. As a consequence, uncertainties can exist due to differences or changes in the methods, or locally lacking data (mainly for private forests which cover 1/3 of the forested area of the Vosges mountains), leading to uneven data quality according to the location. However, our validation is based on a high number of observations (7,300-11,200 management units *per* species), hence a high number of replicates for each of the vulnerability classes, scattered across large ecological gradients. The smallest number of observations was 172 for silver fir for the moderate level of vulnerability, and 286 for Norway spruce for the very low level of vulnerability. This large dataset limits the effect of local uncertainties on the global estimation of map performance.

Conclusion

Our results demonstrate an important impact of recent climate change that increased forest dieback by limiting water availability in Norway spruce stands, and also in silver fir stands to a lesser extent. Vulnerability maps can help to adapt forests to current new climate conditions. Harvesting trees following dieback events causes a financial loss, is a logistical challenge, contributes to pathogen infestation, and creates an important opening up of the environment that modifies microclimates and impairs future reforestation. The massive disappearance of trees could also have significant impacts on biodiversity and human activities by increasing the risk of natural hazards, preventing the preservation of water resources, and altering landscape quality on the long term. We calculated a vulnerability map for the current period; its extrapolation to future conditions remains questionable. The risk of decline will probably be influenced by the evolution of water availability in the next years, and the maps should be updated at regular intervals. In the short term, a potential succession of wet summers might limit dieback. In the long term, increasing temperatures and drought leave little hope for the future of Norway spruce in a large part of the Vosges mountains, where its decline is already widespread. The situation is more contrasted for silver fir, and the evolution of water availability in the coming years will influence its evolution. We can reasonably expect stands with a low level of vulnerability to be spared in the next decades.

Statements & declarations

Fundings

The Unité Mixte de Recherche (UMR) SILVA is supported by a grant overseen by the French National Research Agency (ANR) as part of the 'Investissements d'Avenir' program (ANR-11-LABX-0002-01, Lab of Excellence ARBRE).

Competing Interests

The authors declare no conflict of interest or competing interests.

Author's contribution

D.D. performed the remote sensing analysis, C.B. contributed to the GIS analysis, I.S. and J.C.G. provided bioindicated indices, R.P. provided data from exceptional sanitary cuts, M.L. and C.P. developed the study conception and design, C.P. performed the data collection, realized the analysis and wrote the paper. All of the authors read and corrected the paper, and gave their final approval for publication.

Data availability of data

The datasets analysed during the current study are available from the corresponding author on reasonable request.

REFERENCES

Allen CD, Breshears DD, McDowell NG (2015) On underestimation of global vulnerability to tree mortality and forest die-off from hotter drought in the Anthropocene. Ecosphere 6(8)

Allen CD, Macalady AK, Chenchouni H et al (2010) A global overview of drought and heat-induced tree mortality reveals emerging climate change risks for forests. Forest Ecology and Management 259(4):660-684

Anderson RG, Canadell JG, Randerson JT et al (2011) Biophysical considerations in forestry for climate protection. Frontiers in Ecology and the Environment 9(3):174-182

Archambeau J, Ruiz-Benito P, Ratcliffe S et al (2019) Similar patterns of background mortality across Europe are mostly driven by drought in European beech and a combination of drought and competition in Scots pine. bioRxiv:551820

Aubin I, Boisvert-Marsh L, Kebli H et al (2018) Tree vulnerability to climate change: improving exposure-based assessments using traits as indicators of sensitivity. Ecosphere 9(2)

Baier P, Pennerstorfer J, Schopf A (2007) PHENIPS - A comprehensive phenology model of Ips typographus (L.) (Col., Scolytinae) as a tool for hazard rating of bark beetle infestation. Forest Ecology and Management 249(3):171-186

Bastin JF, Finegold Y, Garcia C et al (2019) The global tree restoration potential. Science 365(6448):76

Becker M (1987) Bilan de santé actuel et rétrospectif du sapin (Abies alba Mill) dans les Vosges. Etude écologique et dendrochronologique. Annales des Sciences Forestières 44(4):379-402

Bonan GB (2008) Forests and climate change: Forcings, feedbacks, and the climate benefits of forests. Science 320(5882):1444-1449

Bonneau M (1985) Le «nouveau dépérissement» des forêts. Symptômes, causes possibles, importance éventuelle de la nature des sols. Revue Forestière Française XXXVI(4): 239-251

Bouvarel P (1984) Le déperissement des forêts attribué aux dépôts atmosphériques acides. Revue Forestière Française XXXVI(3):173-180

Brandl S, Paul C, Knoke T, Falk W (2020) The influence of climate and management on survival probability for Germany's most important tree species. Forest Ecology and Management 458

Brockerhoff EG, Barbaro L, Castagneyrol B et al (2017) Forest biodiversity, ecosystem functioning and the provision of ecosystem services. Biodiversity and Conservation 26(13):3005-3035

Buras A, Rammig A, Zang CS (2020) Quantifying impacts of the 2018 drought on European ecosystems in comparison to 2003. Biogeosciences 17(6):1655-1672

Carnicer J, Coll M, Ninyerola M, Pons X, Sanchez G, Penuelas J (2011) Widespread crown condition decline, food web disruption, and amplified tree mortality with increased climate change-type drought. Proceedings of the National Academy of Sciences of the United States of America 108(4):1474-1478

Cavazzi S, Corstanje R, Mayr T, Hannam J, Fealy R (2013) Are fine resolution digital elevation models always the best choice in digital soil mapping? Geoderma 195:111-121

Charru M, Seynave I, Morneau F, Rivoire M, Bontemps J-D (2012) Significant differences and curvilinearity in the self-thinning relationships of 11 temperate tree species assessed from forest inventory data. Annals of Forest Science 69(2):195-205

Chen J, Franklin JF, Spies TA (1995) Growing-Season Microclimatic Gradients from Clearcut Edges into Old-Growth Douglas-Fir Forests. Ecological Applications 5(1):74-86

Choat B, Jansen S, Brodribb TJ et al (2012) Global convergence in the vulnerability of forests to drought. Nature 491(7426):752-756

Ciais P, Reichstein M, Viovy N et al (2005) Europe-wide reduction in primary productivity caused by the heat and drought in 2003. Nature 437(7058):529-533

Coops NC, Waring RH (2011) Estimating the vulnerability of fifteen tree species under changing climate in Northwest North America. Ecological Modelling 222(13):2119-2129

Das AJ, Slaton MR, Mallory J, Asner GP, Martin RE, Hardwick P (2022) Empirically validated drought vulnerability mapping in the mixed conifer forests of the Sierra Nevada. Ecological Applications 32(2)

642 Das AJ, Stephenson NL, Flint A, Das T, van Mantgem PJ (2013) Climatic Correlates of Tree Mortality in Water-
643 and Energy-Limited Forests. Plos One 8(7)

644 de Groot M, Ogris N (2019) Short-term forecasting of bark beetle outbreaks on two economically important
645 conifer tree species. Forest Ecology and Management 450

646 Dietze MC, Moorcroft PR (2011) Tree mortality in the eastern and central United States: patterns and drivers.
647 Global Change Biology 17(11):3312-3326

648 Elling W, Dittmar C, Pfaffelmoser K, Rotzer T (2009) Dendroecological assessment of the complex causes of
649 decline and recovery of the growth of silver fir (Abies alba Mill.) in Southern Germany. Forest Ecology and
650 Management 257(4):1175-1187

651 Fielding AH, Bell JF (1997) A review of methods for the assessment of prediction errors in conservation
652 presence/absence models. Environmental Conservation 24(1):38-49

653 Fremout T, Thomas E, Gaisberger H et al (2020) Mapping tree species vulnerability to multiple threats as a
654 guide to restoration and conservation of tropical dry forests. Global Change Biology 26(6):3552-3568

655 Fujita S, Noguchi K, Tange T (2021) Different Waterlogging Depths Affect Spatial Distribution of Fine Root
656 Growth for Pinus thunbergii Seedlings. Frontiers in Plant Science 12

657 Gazol A, Camarero J, Anderegg W, Vicente-Serrano S (2017) Impacts of droughts on the growth resilience of
658 Northern Hemisphere forests. Global Ecology and Biogeography 26(2):166-176

659 Gazol A, Camarero JJ (2016) Functional diversity enhances silver fir growth resilience to an extreme drought.
660 Journal of Ecology 104(4):1063-1075

661 Gegout JC, Hervé JC, Houllier F, Pierrat JC (1998) Using vegetation to predict PH in the Vosges mountains
662 Forests. pp. 17

663 Gegout JC, Hervé JC, Houllier F, Pierrat JC (2003) Prediction of forest soil nutrient status using vegetation.
664 Journal of Vegetation Science 14(1):55-62

665 Guinier P (1959) Trois conifères de la flore vosgienne. Bulletin de la société botanique de France 106(85):168-
666 183

667 Han J, Singh VP (2020) Forecasting of droughts and tree mortality under global warming: a review of causative
668 mechanisms and modeling methods. Journal of Water and Climate Change 11(3):600-632

669 Hartmann H, Moura CF, Anderegg WRL et al (2018) Research frontiers for improving our understanding of
670 drought-induced tree and forest mortality. New Phytologist 218(1):15-28

671 Jaime L, Batllori E, Margalef-Marrase J, Pérez Navarro MÁ, Lloret F (2019) Scots pine (Pinus sylvestris L.)
672 mortality is explained by the climatic suitability of both host tree and bark beetle populations. Forest Ecology
673 and Management 448:119-129

674 King G, Zeng L (2001) Logistic Regression in Rare Events Data. Political Analysis 9:137 - 163

675 Knight KS, Brown JP, Long RP (2013) Factors affecting the survival of ash (Fraxinus spp.) trees infested by
676 emerald ash borer (Agrilus planipennis). Biological Invasions 15(2):371-383

677 Kolb T, Keefover-Ring K, Burr SJ, Hofstetter R, Gaylord M, Raffa KF (2019) Drought-Mediated Changes in
678 Tree Physiological Processes Weaken Tree Defenses to Bark Beetle Attack. Journal of Chemical Ecology
679 45(10):888-900

680 Landmann G, Bonneau M, Adrian M (1987) Le dépérissement du Sapin pectiné et de l'Epicéa commun dans le
681 massif vosgien est-il en relation avec l'état nutritionnel des peuplements ? Revue forestière Française XXXIX
682 (1):5-11

683 Lebourgeois F (2007) Climatic signal in annual growth variation of Silver Fir (Abies alba Mill.) and Spruce
684 (Picea abies Karst) from the French Permanent Plot Network (RENECOFOR). Annals of Forest Science, 64
685 (3):333-343

686 Lebourgeois F, Gomez N, Pinto P, Mérian P (2013) Mixed stands reduce Abies alba tree-ring sensitivity to
687 summer drought in the Vosges mountains, western Europe. Forest Ecology and Management 303:61-71

688 Lehmann A, Overton JM, Leathwick JR (2002) GRASP: generalized regression analysis and spatial prediction.
689 Ecological Modelling 157(2-3):189-207

690 Lévy GB, M. (1987) Le dépérissement du sapin dans les Vosges Rôle primordial du déficit d'alimentation en
691 eau. Annales des Sciences Forestières 44(4):403-416

692 Lu LL, Wang HC, Chhin S, Duan AG, Zhang JG, Zhang XQ (2019) A Bayesian Model Averaging approach for
693 modelling tree mortality in relation to site, competition and climatic factors for Chinese fir plantations. Forest
694 Ecology and Management 440:169-177

695 Lundquist JE (2019) Impacts of Bark Beetles on Ecosystem Values in Western Forests-Introduction. Journal of
696 Forestry 117(2):136-137

697 Manel S, Williams HC, Ormerod SJ (2001) Evaluating presence-absence models in ecology: the need to account
698 for prevalence. Journal of Applied Ecology 38(5):921-931

699 Manion PD (1981) Tree disease concepts. Prentice-Hall

700 Maringer J, Stelzer AS, Paul C, Albrecht AT (2021) Ninety-five years of observed disturbance-based tree
701 mortality modeled with climate-sensitive accelerated failure time models. European Journal of Forest Research
702 140(1):255-272

703 Marini L, Økland B, Jönsson AM et al (2017) Climate drivers of bark beetle outbreak dynamics in Norway
704 spruce forests. Ecography 40(12):1426-1435

705 Mc Cook LJ (1994) Understanding ecological community succession: Causal models and theories, a review.
706 Vegetatio 110:115-147

707 McCarthy JJ, Canziani OF, Leary NA, Dokken DJ, White KS (2001) Climate Change 2001: Impacts,
708 Adaptation, and Vulnerability

709 McCullagh P, Nelder JA (1997) Generalized linear models. Chapman & Hall, London, UK

710 McDowell N, Pockman WT, Allen CD et al (2008) Mechanisms of plant survival and mortality during drought:
711 why do some plants survive while others succumb to drought? New Phytologist 178(4):719-739

712 Mesquita RCG, Delamonica P, Laurance WF (1999) Effect of surrounding vegetation on edge-related tree
713 mortality in Amazonian forest fragments. Biological Conservation 91(2-3):129-134

714 Michel A, Seidling W (2018) Forest Condition in Europe: 2018 Technical Report of ICP Forests. Report under
715 the UNECE Convention on Long-Range Transboundary Air Pollution (CLRTAP). BFW Austrian Research
716 Centre for Forests, Vienna, pp. 128

717 Neumann M, Mues V, Moreno A, Hasenauer H, Seidl R (2017) Climate variability drives recent tree mortality in
718 Europe. Global Change Biology 23(11):4788-4797

719 Obladen N, Dechering P, Skiadaresis G et al (2021) Tree mortality of European beech and Norway spruce
720 induced by 2018-2019 hot droughts in central Germany. Agricultural and Forest Meteorology 307

721 Ols C, Bontemps JD (2021) Pure and even-aged forestry of fast-growing conifers under climate change: on the
722 need for a silvicultural paradigm shift. Environmental Research Letters 16(2):5

723 Ondo I, Burns J, Piedallu C (2017) Including the lateral redistribution of soil moisture in a supra regional water
724 balance model to better identify suitable areas for tree species. Catena 153:207-218

725 Pedersen BS (1998) Modeling tree mortality in response to short- and long-term environmental stresses.
726 Ecological Modelling 105(2-3):347-351

727 Peng CH, Ma ZH, Lei XD et al (2011) A drought-induced pervasive increase in tree mortality across Canada's
728 boreal forests. Nature Climate Change 1(9):467-471

729 Pfeifer EM, Hicke JA, Meddens AJ (2011) Observations and modeling of aboveground tree carbon stocks and
730 fluxes following a bark beetle outbreak in the western United States. Global Change Biology 17(1):339-350

731 Piedallu C, Gégout J-C, Perez V, Lebourgeois F (2013) Soil water balance performs better than climatic water
732 variables in tree species distribution modelling: Soil water balance improves tree species distribution models.
733 Global Ecology and Biogeography 22(4):470-482

734 Piedallu C, Gegout JC (2007) Multiscale computation of solar radiation for predictive vegetation modelling.
735 Annals of Forest Science 64(8):899-909

736 Piedallu C, Gegout JC, Bruand A, Seynave I (2011) Mapping soil water holding capacity over large areas to
737 predict potential production of forest stands. Geoderma 160(3-4):355-366

Piedallu C, Gegout JC, Lebourgeois F, Seynave I (2016) Soil aeration, water deficit, nitrogen availability, acidity and temperature all contribute to shaping tree species distribution in temperate forests. Journal of Vegetation Science 27(2):387-399

Pörtner H-O, Roberts DC, Tignor M et al (2022) IPCC, 2022: Climate Change 2022: Impacts, Adaptation, and Vulnerability. Contribution of Working Group II to the Sixth Assessment Report of the Intergovernmental Panel on Climate Change. (eds.). Cambridge University Press. In Press.,

Preisler HK, Grulke NE, Heath Z, Smith SL (2017) Analysis and out-year forecast of beetle, borer, and drought-induced tree mortality in California. Forest Ecology and Management 399:166-178

Pretzsch H (2005) Stand density and growth of Norway spruce (Picea abies (L.) Karst.) and European beech (Fagus sylvatica L.): evidence from long-term experimental plots. European Journal of Forest Research 124(3):193-205

Pretzsch H, Grams T, Haberle KH, Pritsch K, Bauerle T, Rotzer T (2020) Growth and mortality of Norway spruce and European beech in monospecific and mixed-species stands under natural episodic and experimentally extended drought. Results of the KROOF throughfall exclusion experiment. Trees-Structure and Function 34(4):957-970

Pukkala T, Lähde E, Laiho O (2013) Species Interactions in the Dynamics of Even- and Uneven-Aged Boreal Forests. Journal of Sustainable Forestry 32(4):371-403

Rogers Brendan M, Solvik K, Hogg EH et al (2018) Detecting early warning signals of tree mortality in boreal North America using multiscale satellite data. Global Change Biology 24(6):2284-2304

Rotzer T, Haberle KH, Kallenbach C, Matyssek R, Schutze G, Pretzsch H (2017) Tree species and size drive water consumption of beech/spruce forests - a simulation study highlighting growth under water limitation. Plant and Soil 418(1-2):337-356

Roulleau (1912) Bulletin trimestriel de l'office forestier du centre et de l'Ouest tome 3(1ere série)

Rouse WR, Wilson RG (1969) Time and Space Variations in the Radiant Energy Fluxes Over Sloping Forested Terrain and Their Influence on Seasonal Heat and Water Balances at a Middle Latitude Site. Geografiska Annaler: Series A, Physical Geography 51(3):160-175

Schelhaas MJ, Nabuurs GJ, Schuck A (2003) Natural disturbances in the European forests in the 19th and 20th centuries. Global Change Biology 9(11):1620-1633

Senf C, Buras A, Zang CS, Rammig A, Seidl R (2020) Excess forest mortality is consistently linked to drought across Europe. Nature Communications 11(1)

Senf C, Pflugmacher D, Zhiqiang Y et al (2018) Canopy mortality has doubled in Europe's temperate forests over the last three decades. Nat Commun 9(1):4978

Sinclair WA (1965) Comparisons of recent declines of white ash, oaks, and sugar maple in northeastern woodlands. Cornell Plant 20:62-67

Staupendahl K, Zucchini W (2011) Estimating survival functions for the main tree species based on time series data from the forest condition survey in Rheinland-Pfalz, Germany. Allgemeine Forst Und Jagdzeitung 182(7-8):129-145

Suarez ML, Ghermandi L, Kitzberger T (2004) Factors predisposing episodic drought-induced tree mortality in Nothofagus - site, climatic sensitivity and growth trends. Journal of Ecology 92(6):954-966

Sun JB, Yang JY, Zhang C, Yun WJ, Qu JQ (2013) Automatic remotely sensed image classification in a grid environment based on the maximum likelihood method. Mathematical and Computer Modelling 58(3-4):573-581

Taccoen A, Piedallu C, Seynave I et al (2019) Background mortality drivers of European tree species: climate change matters. Proceedings of the Royal Society B-Biological Sciences 286(1900)

Thomas AL, Gegout JC, Landmann G, Dambrine E, King D (2002) Relation between ecological conditions and fir decline in a sandstone region of the vosges mountains (northeastern France). Annals of Forest Science 29:265-273

Thornthwaite CW, Mather JR (1955) The water balance. Laboratory of Climatology, Publication in Climatology. n°8

Torssonen P, Strandman H, Kellomaki S et al (2015) Do we need to adapt the choice of main boreal tree species in forest regeneration under the projected climate change? Forestry 88(5):564-572

Turc L (1961) Estimation of irrigation water requirements, potential evapotranspiration: a simple climatic formula evolved up to date. Ann Agron 12(1):13-49

Urli M, Porté AJ, Cochard H, Guengant Y, Burlett R, Delzon S (2013) Xylem embolism threshold for catastrophic hydraulic failure in angiosperm trees. Tree Physiology 33(7):672-683

van Mantgem PJ, Stephenson NL, Byrne JC et al (2009) Widespread Increase of Tree Mortality Rates in the Western United States. Science 323(5913):521-524

Verbesselt J, Robinson A, Stone C, Culvenor D (2009) Forecasting tree mortality using change metrics derived from MODIS satellite data. Forest Ecology and Management 258(7):1166-1173

Vitali V, Buntgen U, Bauhus J (2017) Silver fir and Douglas fir are more tolerant to extreme droughts than Norway spruce in south-western Germany. Global Change Biology 23(12):5108-5119

Ward NL, Masters GJ (2007) Linking climate change and species invasion: an illustration using insect herbivores. Global Change Biology 13(8):1605-1615

Western AW, Zhou S-L, Grayson RB, McMahon TA, Blöschl G, Wilson DJ (2004) Spatial correlation of soil moisture in small catchments and its relationship to dominant spatial hydrological processes. Journal of Hydrology 286(1):113-134

Williams AP, Allen CD, Macalady AK et al (2013) Temperature as a potent driver of regional forest drought stress and tree mortality. Nature Climate Change 3(3):292-297

Supporting information

Id	Silver fir	Norway spruce
1	+95% Silver fir	+95% Norway spruce
2	≥50% silver fir, + Norway spruce and others	≥50% Norway spruce, + silver fir and others
3	≥50% silver fir, + others; no Norway spruce	≥50% Norway spruce, + others; no silver fir
4	<50% silver fir, + Norway spruce and others	<50% Norway spruce, + silver fir and others
5	<50% silver fir, + others; no Norway spruce	<50% Norway spruce, + others; no silver fir
6	<5% silver fir	<5% Norway spruce
7	Young stands	Young stands

Table S1: *Evaluation of mixture classes for the silver fir and Norway spruce stands.*

812

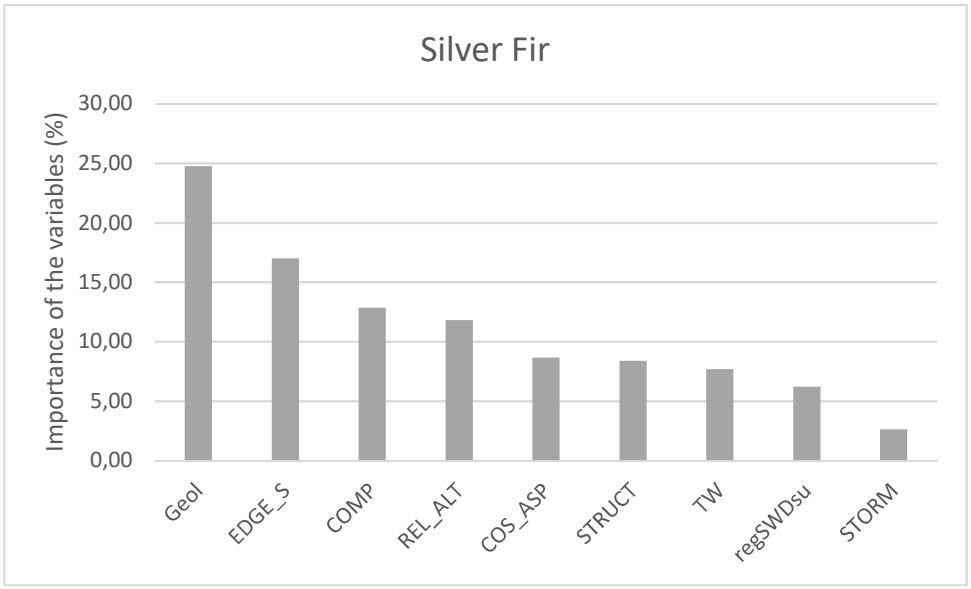

813

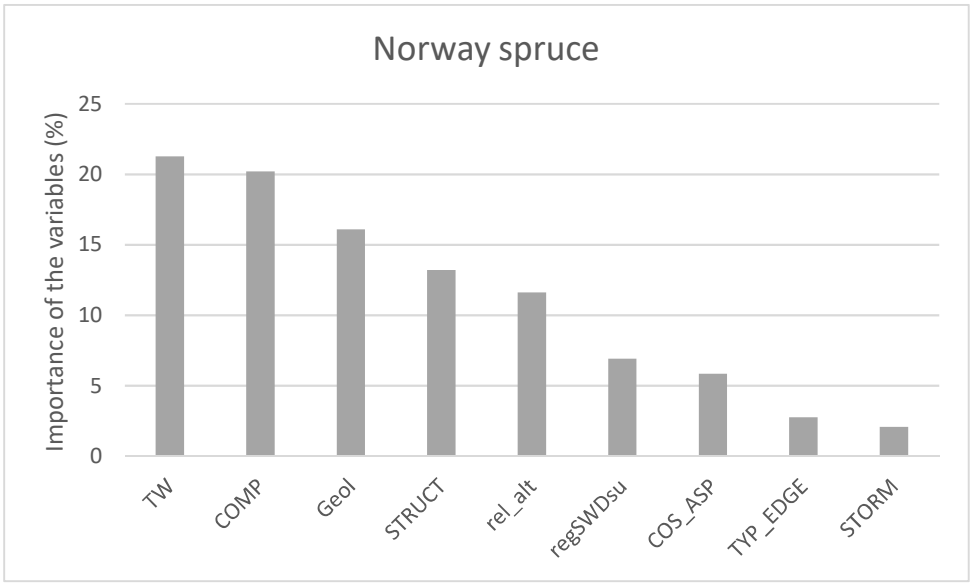

814

815 **Figure S1***: Relative importance of the variables selected in the silver fir and Norway spruce models.*

816

Variable	Modalities for qualitative variables	Coefficient	Coefficient ^2
Intercept		-2.3462	
REL_ALT		2.9993	- 1.6372
COS_ASP		-0.4539	-0.4225
RegSWD_su		0.7869	
TW		27.2816	
GEOL	Principal conglomerate and acidic granite	0	
	Quaternary deposits, granites, sandstones little acidic	-0,8239	
	Voltzia sandstone, metamorphic rocks, acidic deposits	-1,8119	
	Acidic Vosges sandstone	-0,6203	
	Neutral magmatic and metamorphic rocks	-0,2841	
	Neutral to basic rocks and migmatite	1,0868	
	Volcanic pyroclastic rock	0,1552	
COMP	Pure silver fir stand	0	
	More than 50% silver fir with Norway spruce	0,1046	
	More than 50% silver fir with broadleave sp.	0,6036	
	Less than 50% silver fir with broadleave sp.	-1,4861	
STRUCT	Even-aged stand	0	
	Young stand	-0,686	
	Uneven-aged stand	-0,7077	
STORM	Less than 50% damage	0	
	More than 50% damage	-0,6936	
EDGE_S	Absence of south forest edge	0	
	Presence of south forest edge	1,1293	

Table S2*: Coefficients for the silver fir model.*

Variable	Modalities for qualitative variables	Coefficient	Coefficient ^2
Intercept		1.3578	
REL_ALT		1.1820	
COS_ASP		-0.4005	
RegSWD_su		0.7660	
TW		33.8845	
GEOL	Granites, quaternary deposits, primary	0	
	Granodiorites, migmatic rocks, sedimentary neutral to acidic	-1,1875	
	Voltzia or shells sandstone, magmatic, volcanic	0,6745	
	Vosges or intermediate sandstone, granits, gneiss	-0,2069	
	Magmatic basic rock	-0,4483	
	Sedimentary basic rock	2,4633	
COMP	Pure Norway spruce stand	0	
	More than 50% Norway spruce with Silver fir	-0,9841	
	More than 50% Norwauy spruce with broadleave sp.	-1,1953	
	Less than 50% Norway spruce with broadleave sp.	-2,0768	
STRUCT	Even-aged stand	0	
	Young stand	-1,0156	
	Uneven-aged stand	-0,5555	
STORM	Less than 50% damage	0	
	More than 50% damage	-0,825	
EDGE	Absence of forest edge	0	
	Presence of edge between two stands	0,5407	
	Presence of edge with an open environment	0,2568	

827

828 **Table S3***: Coefficients for the Norway spruce model.*

829

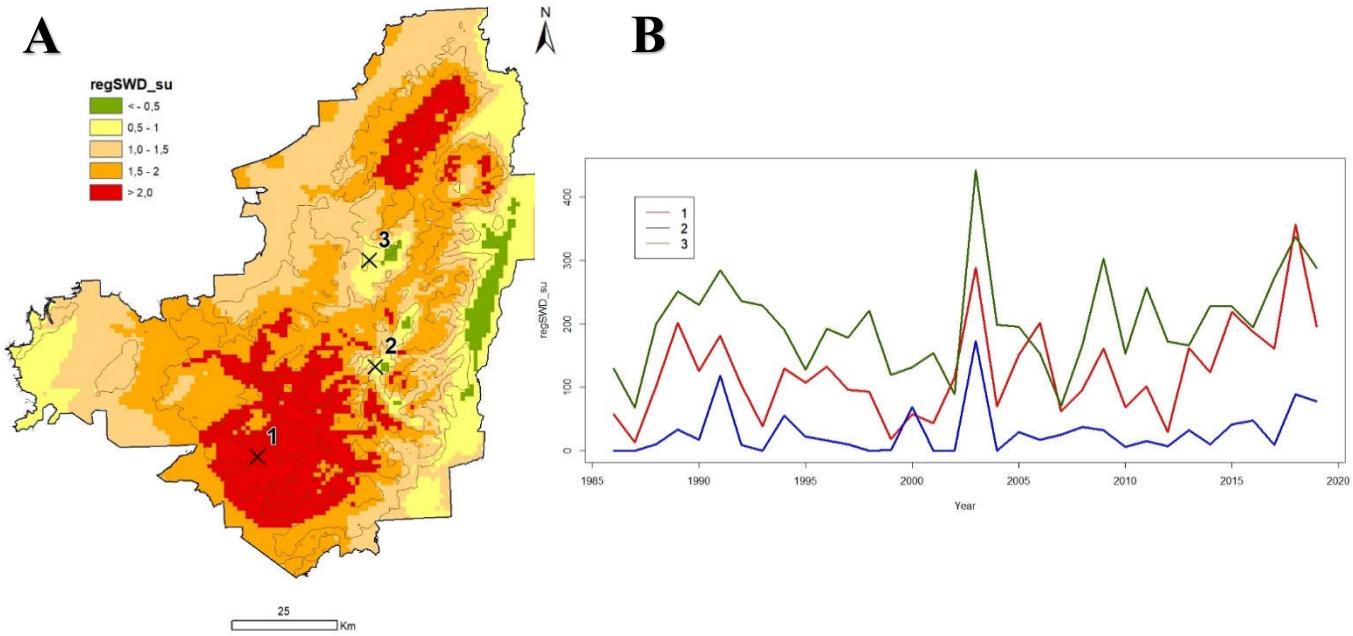

830

831 **Figure S2:** Comparison of the summer SWD trend (variable regSWD_su) for three contrasted locations over the
832 1986-2019 period: A) map of summer SWD trends and localisation of the three time series, B) summer SWD
833 time series for the 1986-2019 period. Vulnerability was most important in site n°1 (regSWDsu > 2), where the
834 time series showed a substantial increase of water stress from 2012, with a high probability of dieback (0.70 and
835 0.78 for silver fir and Norway spruce respectively, see figures 5 and 6). Site n°3 showed similar water stress
836 levels from 2012, but a higher one than site n°1 between 1986 and 2012. The probability of dieback was much
837 lower (0.15 and 0.30 for silver fir and Norway spruce, respectively), suggesting that trees were more adapted to
838 drought than in site n°1. Site n°2 was at a higher altitude, with little moisture stress and a low level of risk
839 despite a slight increase of the water deficit from 2015 (probability of dieback: 0.15 and 0.30 for silver fir and
840 Norway spruce, respectively).

841

842